Future distribution of early life stages of small pelagic fishes in the northwestern Mediterranean

Authors: F. Maynou[1*], A. Sabatés[1], E. Ramírez Romero[2], I. A. Catalán[2], V. Raya[1]

Affiliation:

1: Institut de Ciències del Mar, CSIC, Psg. Marítim de la Barceloneta 37-49, 08003 Barcelona

2: IMEDEA, CSIC-UIB, c. Miquel Marquès 21, 07190 Esporles

* contact author : maynouf@icm.csic.es ORCID: https://orcid.org/0000-0001-7200-6485

anas@icm.csic.es http://orcid.org/0000-0002-0315-6444

eramirez@imedea.uib-csic.es https://orcid.org/0000-0002-7228-6939

ignacio@imedea.uib-csic.es ORCID: https://orcid.org/0000-0002-6496-9182

vraya@icm.csic.es http://orcid.org/0000-0002-5791-540X

running head: Future distribution of early life stages.

Abstract

We studied the effect of climate change on the potential spawning habitats of two marine small pelagic fishes. We examined the projected changes in the potential spawning habitat of the summer-spawning anchovy (*Engraulis encrasicolus*) and round sardinella (*Sardinella aurita*) in the northwestern Mediterranean by combining the regionalized projections of RCP scenarios with an existing species distribution model (SDM). The SDM was based on a separate generalized additive model for the eggs and larvae of the two species computed from ichthyoplankton sampling that was conducted with simultaneous readings of surface temperature, salinity and chlorophyll-*a* values as predictor variables. The SDM was projected for the 2010 decade, which represented the present-day conditions, with these environmental variables obtained from the regionalized POLCOMS-ERSEM biogeochemical model forced by the RCP 4.5 and RCP 8.5 scenarios. The comparison of the present-day projection results with the projections for the middle and final decades of the 21st century showed that the suitability of the spawning habitat as defined by the anchovy eggs model was likely to increase over time under RCP4.5 or decrease slightly under RCP8.5, but the habitat for anchovy larvae was likely to decrease in all cases. Loss of habitat was projected to be particularly important in the south of the study area on the Ebre River delta continental shelf. Conversely, the probability of round sardinella occurrence will significantly increase under both scenarios. The potential habitat of this species, which is of subtropical origin, is likely to shift northwards. The limitations of the existing models to extrapolate the current results to future scenarios are discussed regarding i) the uncertainty in the projections of driving environmental variables (e.g., chlorophyll-*a*), ii) the simplified nature of the projection models, which did not capture the dynamics of the early life stages of the fish at a small scale, and iii) insufficient consideration of important drivers, such as larval transport or retention by mesoscale hydrographic phenomena.

keywords:

Anchovy, Round sardinella, climate change, Northwestern Mediterranean, RCP scenarios, eggs, larvae

1 Introduction

The oceanographic conditions of the northwestern Mediterranean permit the existence of local, high productivity areas in an oligotrophic sea (Estrada 1996; Siokou-Frangou et al. 2009). In particular, river outflow from the main two rivers in the area, the Rhône in the Gulf of Lions and the Ebre on the eastern seaboard of the Iberian Peninsula (Fig. 1), allows for high localized productivity in the area where small pelagic species spawn (Palomera et al. 2007). In the area, two winter-spawning small pelagics, sardine (*Sardina pilchardus*) and sprat (*Sprattus sprattus*), coexist with two summer-spawning species, anchovy (*Engraulis encrasicolus*) and round sardinella (*Sardinella aurita*) (van Beveren et al. 2016; Sabatés et al. 2013). The latter two species show peak spawning activity during the summer months, when pelagic productivity is generally at the lowest levels, but their larvae can feed on high productivity patches on the surface in the vicinity of the major river outflow or at 50-60 m in depth, where the deep chlorophyll maximum (DCM) occurs (Olivar et al. 2001; Sabatés et al. 2013). In recent decades, good knowledge of the spawning habitats of *E. encrasicolus* and *S. aurita* and their variation over time has been gathered in the northwestern Mediterranean (Palomera et al. 2007; Maynou et al. 2020). Their spawning success and consequent recruitment are known to be threatened by hydrological changes caused primarily by increased temperature and decreased primary productivity (Sabatés et al. 2013; Maynou et al. 2014.

Changes in the abundance and distribution of marine species in response to climate change in recent decades have been well documented. In European Atlantic waters, for instance, a distributional shift towards higher latitudes in relation to ocean warming has been shown for fish and invertebrate assemblages in the North Sea (Dulvy et al. 2008; Hiddink et al. 2015). Beyond a certain critical threshold of temperature, salinity or pH, less tolerant species will move away or disappear from areas where they were historically abundant to be replaced by species that were rare or altogether new. In the Mediterranean, for instance, a northward shift of warm water species from the southern Mediterranean has been reported ("meridionalization": CIESM 2008; Sabatés et al. 2009; Durrieu du Madron et al. 2011), as well as the ongoing substitution of native fish fauna by Lessepsian migrants, particularly in the eastern Mediterranean (Azzurro et al. 2011). In the absence of detailed information on the physiological response of marine organisms to environmental changes (Catalán et al. 2019) or integrated ecosystem models (Peck et al. 2018), empirical models relating environmental covariates with species distribution are useful tools for attempting to anticipate these faunal redistributions (Planque et al. 2011; Elith and Leathwick 2009).

Statistical models of organism distributions seek to associate environmental conditions with species presence or abundance (Planque et al. 2007, 2011). These models, which are also referred to as habitat

models (Guisan and Zimmermann 2000), habitat suitability models (Hirzel et al. 2006) or species distribution models (SDM; Guisan and Thuiller 2005), have been used to describe the (current) potential spawning habitat of small pelagic fish (Planque et al. 2011; Giannoulaki et al. 2013). However, these models cannot, by their very nature, capture the true realized spatial distribution of a species, which is usually modulated by other factors, such as biological interactions or fisheries exploitation (Planque et al. 2011). SDMs are nevertheless useful for modelling species responses to environmental changes, such as those projected by climate change models over the coming decades. Small pelagic fish are a good case study for understanding the impact of climate change on marine fishes due to their relatively short life span and the dependence of their populations on spawning/recruitment success, which results in fluctuating populations (Checkley et al. 2009). Spatial and temporal fluctuations in abundance can usually be linked to changes in a few key environmental variables, such as water temperature, salinity, biological productivity or oceanographic structures (Nevárez-Martínez et al. 2001; Planque et al. 2007; Brown et al. 2011).

In the northwestern Mediterranean, important changes in abundance and spatial distribution have already been documented for the dominant four small pelagics (Sabatés et al. 2009, Coll et al. 2018). Palomera et al. (2007) and van Beveren et al. (2016) showed that the abundance of the two target species in the fishery (sardine and anchovy) has decreased over the last few decades along the Spanish and French coasts. Conversely, the abundance of the two low-value species, sprat and round sardinella, has increased since the early years of the current century. Although intense fisheries exploitation is partly to blame for these (and other) ecosystem changes (cf. Taboada and Anadón 2016), the roles of increasing water temperature, decreasing river runoff, or atmospheric drivers, such as the North Atlantic Oscillation or the western Mediterranean Oscillation, have been demonstrated (Martín et al. 2012; Brosset et al. 2015; van Beveren et al. 2016). Other indicators of the influence of climate change on oceanographic conditions in the area are the decreasing biological productivity (cf. Colella et al. 2016, who used satellite-derived chlorophyll-*a* as a proxy) or the expected increase in stratification and deepening of the DCM (Durrieu du Madron et al. 2011; Coma et al. 2009), but these and other potential drivers have not been used in correlative analysis of the spatial distribution of small pelagics in the area.

Our objectives were to map the future potential spawning habitat ("habitat where the environmental conditions are suitable for spawning", Planque et al. 2007) of anchovy and round sardinella in the northwestern Mediterranean. We applied a regression model of the realized spawning habitat of the early life stages (eggs and larvae) that was parameterized with empirical hydrographic data and coupled with climate model projections for the middle and final decades of the 21st century that were obtained from the regionalized POLCOMS-ERSEM model (Kay et al. 2018).

2 Material and Methods

2.1 Study area

The study area covered the Catalan Sea continental shelf and the slope from 40 to 42.5º N latitude and from near the coast to 1000 m depth (Fig. 1). This area of the northwestern Mediterranean is characterized by a narrow continental shelf, which becomes wider in the southernmost area (in the vicinity of the Ebre River delta) and in the north (between the main submarine canyons), as well as, notably, in the Gulf of Lions. The general surface circulation in the region was well established with a main shelf-slope current, the Northern Current, which moves from northeast to southwest along the continental slope (Millot 1999). The Northern Current is subjected to high mesoscale variability that causes oscillations, meandering and eddy generation (Sabatés et al. 2013, 2018). The input of continental water plays an important role in this region. The southern shelf receives a significant river outflow from the Ebre River, while the northern area is affected by the outflow of the Rhône River, which is the largest river in the western Mediterranean basin and outflows into the Gulf of Lions. The northern sector, which is more directly influenced by strong northerly winds, is generally colder than the central and southern parts, and a surface thermal front, which exists between 41 and 42°N, is perpendicular to the coast and roughly coincides with the limit of frequent northerly winds (Sabatés et al. 2009).

The water column structure is characterized by a marked seasonal cycle, with strong stratification in summer, which results in limited vertical water movement and practical depletion of surface nutrients. In summer, primary production is mostly restricted to the DCM, a thin layer at the deepest levels of the photic zone (50-60 m depth, Estrada et al. 1993). In that period, the surface productivity is limited to areas under the influence of river runoff, which are identifiable by lower salinity down to ~ 20-30 m, above the thermocline (Salat et al. 2002).

2.2 Species distribution model

We estimated the future potential spatial distribution of the early life stages of the two summer-spawning small pelagic fish (anchovy and round sardinella) based on a regression model parameterized with ichthyoplankton survey data and *in situ* environmental data (Maynou et al. 2020) to delineate the habitat where the environmental conditions will be suitable for spawning (Fig. 2). The sampling stations are shown in Fig. 1, and field sampling is described in Annex 2 of the Electronic Supplementary Material (ESM) (see Sabatés et al. 2018 for full details). The regression model is a generalized additive model (GAM) that relates the abundance of anchovies and the presence of the early life stages of round sardinella to surface water conditions (temperature, salinity, chlorophyll-*a*) in the summer months with peak spawning (June and July). These variables are good descriptors of the spawning habitat and larval environment of both species in the study area (Palomera et al. 1997;

Maynou et al. 2014). Briefly, Maynou et al. (2020) estimated the spatial distribution of the early life stages of anchovy and round sardinella from the ichthyoplankton survey data obtained in three summer sampling programmes, which occurred in 1983, from 2003-2004 and from 2011-2012, where ichthyoplankton were sampled simultaneously with hydrographic data on a grid of stations (Fig. 1). In the case of anchovy, the regression GAM model is a predictor of the abundance ($n \cdot 10\ m^{-2}$) of eggs and larvae and uses a quasi-Poisson distribution function and logarithmic transformation of the dependent variable. For round sardinella, due to the high number of absences in the data, only the probability of occurrence was modelled based on a GAM model with a binomial distribution function and logit transformation. The model coefficients were reproduced here in Table S1. Note that the coefficients of the spline smoother that were larger than 1.0 represent non-linear relationships between the environmental predictor and the outcome. The coefficients equal to 1.0 in the round sardinella egg model (chlorophyll-*a* and salinity) indicate linear relationships at the scale of the predictor. A detailed interpretation of the partial effects of the predictors is given in Maynou et al. (2020), but in summary, the model coefficients show that anchovy eggs and larvae are more abundant at water temperatures between 22 and 24 ºC, salinities of 37.25 to 37.75 and chlorophyll-*a* concentrations of 0.14–0.22 mg m^{-3}. The presence of round sardinella eggs was enhanced by chlorophyll-*a* higher than 0.20 mg m^{-3} and salinity lower than 37.5, while the effect of temperature reached a maximum at approximately 25 ºC. For round sardinella larvae, chlorophyll-*a* was not retained in the model, and salinity had an effect comparable to that on the eggs, while the effect of temperature was positive in the range 24–27.2 ºC (maximum temperature observed).

2.2.1 Biogeochemical model

The environmental data (sea surface temperature, SST; sea surface salinity, SSS; and sea surface chlorophyll-*a*; CHL) in the 2006-2015 (referred to herein as the 2010s or current environmental conditions), 2041-2060 (referred to as the 2050s) and 2080-2099 (referred to as the 2090s) periods were obtained from the POLCOMS-ERSEM modelling system (Holt et al. 2012; Kay and Butenschön 2018).

POLCOMS (the Proudman Oceanographic Laboratory Coastal Ocean Modelling System, Holt and James 2001) is a 3-D physical model able to capture the oceanographic dynamics of both the deep ocean and the continental shelf. ERSEM (European Regional Sea Ecosystem Model) is a complex marine biogeochemical model that includes bacteria, four phytoplankton and three zooplankton functional groups, variable carbon to chlorophyll-*a* ratios and independent nutrient pools for carbon, nitrogen, phosphorous and silicate (Holt et al. 2010; Butenschön et al. 2016). The POLCOMS-ERSEM coupled model framework was regionalized and used at a 10-km spatial resolution and for 40

sigma layers in the NE Atlantic and Mediterranean basins. Subsequently, the coupled model was subregionally validated with surface data (Kay and Butenschön 2018; Ciavatta et al. 2019).

Within the frame and efforts of an EU project (CERES; https://ceresproject.eu/), projections were made for the Representative Concentration Pathway RCP4.5 and RCP8.5 greenhouse gas scenarios using data from the global climate model MPI-ESM-LR (http://www.mpimet.mpg.de/en/science/models/mpi-esm.html) and downscaled to a regional climate model. RCP4.5 and RCP8.5 represent moderate and high greenhouse gas concentrations that increase radiative forcing on Earth by 4.5 W m^{-2} and 8.5 W m^{-2} at the end of the 21st century, respectively (Alexander et al. 2018). The model was provided by the Plymouth Marine Laboratory (PML, UK) (Kay et al. 2018). The projections of the riverine discharge and nitrogen and phosphorus loadings used the E-HYPE v3.2 with the same global climate model and a business-as-usual nutrient scenario. The river models were made available by the Swedish Meteorological Office (SMHI) (https://www.smhi.se/en/research/research-departments/hydrology/hype-1.7994). The coupled model was run using both scenarios for the 2006-2099 period, and weekly outputs were saved for the present study.

For each of the three environmental variables (SST, SSS, CHL), the climatological values corresponding to June-July were extracted over a rectangle covering the study area (bounded by 0.4 – 4º E and 40 - 42.5º N) for 2006-2015 (representing the 2010s decade), mid-21st century (2041-2060, coded as the 2050s) and the end of the 21st century (2080-2099, coded as the 2090s). In addition, the standard error of the mean of the model predictions was calculated for each grid cell. We chose a 10-yr portion of the data for the "present-day" period (i.e., the decade 2010s) starting in 2006 because we had observational data of the environmental variables and early life stages for the summers of 2011 and 2012 from Fishjelly cruises (Sabatés et al. 2018), which bracketed the middle of the 2006-2015 period. This period served both as a baseline for comparison with future changes and to compare the present-day projections of the biogeochemical models with actual observations during the ichthyoplankton surveys.

2.2.2 Bias correction for the projections

POLCOMS-ERSEM model reasonably captured the main oceanographic features of the study area (Sabatés et al. 2013, 2018; Kay et al. 2018), but the SST was generally overestimated in the lower range (below 21.5 ºC) and underestimated in the upper range (above 23 ºC) (ESM Annex 1). The SSS was generally overestimated, particularly for the percentiles above 50% (approx. 38.75 psu), but the bias decreased for the percentiles above 90% (ESM Annex 1). The CHL represented the worst case of mismatch between field observations from the 2011-2012 cruises and the POLCOMS-ERSEM model.

Even if the general picture of high chlorophyll-*a* in the Ebre delta can be detected, the values produced by the POLCOM-ERSEM model were 2-3x higher than observed, and the bias actually increased with increasing values of chlorophyll-*a* (ESM Annex 1). The model predicted high values of chlorophyll-*a* in the northern half of the study area and in the Gulf of Lions that were not observed in summer. Note that the bias problems were practically identical under the RCP4.5 and RCP8.5 scenarios.

The values of the environmental variables were corrected for bias by means of quantile linear transformation (Gudmundsson et al. 2012, *qmap* library in R v. 3.5.0) of the original values to match the data distribution of the observed *in situ* values during the ichthyoplankton sampling surveys in the summers of 2011 and 2012 (Sabatés et al. 2018) (ESM Annex 1). For each variable and grid cell, the difference between the original POLCOMS-ERSEM 2006-2015 projection ("current") and the bias-corrected map was computed ("delta values", following the quantile linear transformation method in Gudmundsson et al. 2012). These delta values were subtracted from each corresponding map cell representing the future conditions (2050s and 2090s).

2.2.3 Projection of eggs and larvae

For each cell in the study area, the GAM developed by Maynou et al. (2020) was applied to the bias-corrected climatological environmental variables (SST, SSS, CHL) to compute the value of the eggs or larvae of anchovy and round sardinella, which were averaged over each period, for the current (2010s) and future (2050s, 2090s) conditions (Fig. 2). To determine the error in the estimate, the standard error of the mean (S.E.M.) was computed as follows: i) for each environmental variable and grid cell, 1000 values were randomly produced from the climatological and standard deviation values; ii) for each grid cell, the GAM predictor was applied over the 1000 values, yielding 1000 estimates of S.E.M.; iii) the average of the S.E.M. values was used to produce maps of the precision of the estimates. The computations to project the habitats of the early life stages of both species were carried out with functions in the libraries ncdf4, HiClimR, mgcv and qmap in R (v. 3.5.0).

3 Results

3.1 Projection of environmental variables

3.1.1 Current conditions (2006-2015)

ESM Annex 1 shows the spatial distribution of the climatological values of the three environmental variables that were used to define the small pelagic potential habitat, corresponding to current conditions, which are representative of the 2010s, in the two projection scenarios. Overall, the bias-corrected maps for the current conditions reproduced the average environmental gradients observed during the cruises reasonably well (Sabatés et al. 2013, 2018). The bias-corrected maps showed a

south to north gradient of temperature, with the colder temperatures in the northern area (approximately 20-21ºC) but also in the waters influenced by the Ebre River outflow (colder waters of continental origin). Temperature was predicted to be slightly lower in the northern sector under the RCP8.5 scenario. The bias-corrected salinity maps showed a clear shallow-deep gradient with the lowest salinities over the southern area and in the northernmost part (values approximately 37.4-37.6) in both areas influenced by freshwater of continental origin (from the Ebre and Rhône, respectively), with little difference between scenarios. With regard to the surface chlorophyll-*a*, the values of the bias-corrected maps in the 2010s were projected to be very low (typically <0.1 mg m^{-3}) everywhere, corresponding to a summer situation in Mediterranean waters with very low surface productivity, except in the southern area influenced by outflow of the Ebre River (0.25-0.3 mg m^{-3}) and near the coast in the northernmost part influenced by the Rhône River outflow. In the RCP8.5 scenario, the bias-corrected chlorophyll-*a* was overall predicted to be lower than in RCP4.5.

3.2 Future conditions (2050s, 2090s)

The environmental conditions derived from the biogeochemical model for RCPs 4.5 and 8.5 in the central and final decades of the 21st century are given in Fig. 3. Under RCP4.5 (Fig. 3a, b), temperatures are projected to increase progressively overall in the 2050s and 2090s, but the north-south gradient is expected to remain stable over time, with temperatures lower than 22 ºC to the north of 41.5º. The salinity would not vary markedly between the 2010s (ESM Annex 1) and 2050s, but it would show a significant increase in the 2090s (Fig. 3), likely as a consequence of reduced precipitation. The pattern of surface chlorophyll-*a* is projected to remain stable but to reach higher levels in the northernmost boundary of the study area, which is under the influence of Rhône riverine waters (right panels in Fig. 3). Note that the biogeochemical model projects high chlorophyll-*a* values overall in the northern part of the study area, as mentioned above, which contrasts with the observed current conditions of low surface productivity in the summer months. The quantile regression correction proved to be insufficient to correct for such bias.

In RCP8.5 (Fig. 3c, d), the surface temperature was projected to follow a similar spatial pattern but with higher absolute values than under RCP4.5 (cf. Fig. 3a, Fig. 3c). For the end of the century, surface temperatures below 22º C are expected to be found only northwards of 42º N. Salinity in 2050 would be overall higher than present, except in the northernmost continental shelf where values closer to the current climatological average are expected. In 2090, salinity increases significantly in the northern half of the study area but is projected to be relatively low offshore of the continental shelf of the Ebre delta. Under RCP8.5, chlorophyll-*a* is expected to show lower values than the current climatological averages in the southern half of the study area, but as in RCP4.5, the chlorophyll-*a*

values in the northern area appear unrealistically high, and the suspected bias could not be successfully corrected with the quantile regression model.

The boxplots in Fig. 4 summarize the range of projected values of the environmental variables. Temperature projections under the two scenarios differ markedly, although an overall increase is predicted, higher for RCP8.5 than for RCP4.5, as can be expected. Salinity is expected to reach overall higher values in RCP4.5 than in RCP8.5 in the 2090s. Chlorophyll-*a* is projected to be higher in any future scenario than current bias-corrected values of approximately 0.1 mg m^{-3}, although scenario 4.5 systematically projects higher chlorophyll-*a* than RCP8.5. In the RCP4.5 scenario,chlorophyll-*a* would reach its highest value in the 2050s and decrease in the 2090s, while the average chlorophyll-*a* under RCP8.5 would be closer to the present values. Note, however, the large variability of the chlorophyll-*a* projections for both future scenarios.

3.3 Projections of early life stages

3.3.1 Current conditions (2006-2015)

ESM Annex 2 shows the observed spatial distribution of anchovy and round sardinella early life stages during the 2011-2012 summers from field ichthyoplankton sampling. Anchovy eggs were mainly located over the Ebre shelf and in the northern part of the area, while larvae showed a wider distribution being more abundant in the northern half of the study area. Note differences in the spatial distribution between 2011 (June) and 2012 (July): In the latter, the early life stages were located more offshore of the Ebre River continental shelf, and the two northernmost transects were not sampled. Round sardinella showed a patchier distribution, eggs were preferentially located very close to the coast, and larvae showed a wider distribution extended offshore.

Fig. 5 shows the maps of the distribution of early life stages for anchovy and round sardinella in the baseline period (2010s) under the two RCPs. In general, the projections of the spatial distribution of early life stages of both species are not markedly different between scenarios in the baseline period. Eggs and larvae of anchovy are predicted to be more abundant at present in waters offshore of the Ebre River delta, the central coast and offshore of the northern sector. Comparing the projections in Fig. 5 with the observations of anchovy eggs and larvae during the summer 2011-2012 cruises (ESM Annex 2), we observe that the general distribution pattern is well captured by the models, except in the grid cells near the coast in the Ebre delta and adjacent to the Gulf of Lions, where abundance is projected to be very low. Eggs and larvae of round sardinella in the field samplings showed a high degree of patchiness but were mostly localized in the southern half of the study area (ESM Annex 2). In the model, round sardinella eggs are projected to be more abundant immediately adjacent to the Ebre River delta, while the habitat for larvae extends further northwards to approximately 41.5º N latitude (Fig. 5).

3.3.2 Future distribution (2050s, 2090s)

Under RCP4.5, the abundance of anchovy eggs is projected to increase from approximately 400 · 10 m^{-2} estimated for the 2010s to be over 500 · 10 m^{-2} (Fig. 6a). In RCP8.5, the results show that egg abundance would increase in the 2050s but decrease to values slightly lower than the current values for the 2090s (Fig. 6a). However, under both future scenarios, the abundance of larvae would be lower than at present, suggesting that even if conditions for spawning can remain constant or even improve in the future, larval habitat is likely to shrink (Fig. 6b). In the case of round sardinella, the probability of occurrence of both eggs and larvae is expected to have a large increase in both scenarios.

The maps of the suitability differences between the 2050s and 2010s and the 2090s and 2010s under RCP4.5 and RCP8.5 are shown in Figs. 7 and 8, respectively (ESM Annex 3 for projected absolute values). Under RCP4.5, the potential spawning habitat of anchovy, as measured by the distribution of eggs, was not projected to vary significantly spatially, although higher occupancy is projected for the continental shelf immediately adjacent to the Ebre delta and relatively lower densities in the northern part of the area (Fig. 7). However, a reduction in the suitability of the habitat in the southern area, which is offshore of the Ebre delta, is projected for larvae. This was particularly accentuated under RCP8.5 for the 2090s (Fig. 8). Under RCP8.5, the projections for larvae suggest higher abundance on the northern half (north of 41.5º N) of the study area than those projected by RCP4.5. The difference maps for the anchovy in Figs. 7 and 8 show how habitat suitability would increase in areas adjacent to the coast (in shallower water, especially near the Ebre River delta). This effect is even clearer for larvae, which would actually increase only in the coastal waters immediately adjacent to the Ebre delta and in the northernmost part.

In the case of round sardinella, the figures in ESM Annex 3 show that the probability of finding eggs and larvae is very low north of approximately 41.75º N, but there are important differences between the projections for eggs or larvae. Under both scenarios, eggs are projected to distribute northwards well beyond the current range around the Ebre delta continental shelf (cf. ESM Annex 3 and Fig. 5). In the 2090s under RCP8.5, round sardinella eggs are projected to be found even in the Gulf of Lions area (but note the very low probability to the south and west of the Ebre continental shelf). The probability of finding larvae of round sardinella will not vary spatially between either scenario and the current conditions (i.e., from approximately 40º to 41.75º N), but the probability values will be significantly higher than 0.5 in many areas, whereas at present, the probabilities higher than 0.5 were only estimated for the areas immediately south and west of the Ebre River.

The projected spatial error of the mean estimate (ESM Annex 4) suggests higher uncertainty in the offshore stations and to the south of the study area, particularly for the anchovy larvae and in the 2090 scenarios. For round sardinella, the standard error of mean occurrence was generally low(below 0.15), suggesting that the results had high confidence.

4 Discussion

4.1. Biogeochemical projection model

The POLCOMS-ERSEM biased-corrected model projections showed increased SST under both scenarios; these changes would be larger under RCP8.5 than under RCP4.5 and reaching higher values by the end of the 21st century (Fig. 4a). The projected increases were naturally in accordance with the global ensemble models because this biogeochemical model is based on a regionalization of the CMIP5 projections, which suggest an average SST increase of approximately 0.4 °C per decade and identify the Mediterranean Sea as the European Sea with the most extreme projected warming (Alexander et al. 2018). However, this temperature increase is projected to show important spatial differences, with lower increases in the northern half of the study area, close to the Gulf of Lions, which agrees with the historically different thermal regimes at that spatial scale during the summer months (Pastor et al. 2018). Salinity (bias-corrected) is expected to increase compared to the present conditions under both scenarios and more acutely towards the end of the century for RCP4.5, particularly offshore (Fig. 4b). The most recent reanalyses of the climatic trends in salinity show an increase in the area at different depths (Iona et al. 2018), but the sources of uncertainty associated with these projections (including river discharges) suggest that they should be interpreted with caution. The projections of surface chlorophyll-*a* presented even higher uncertainties than salinity for our study area. Although the (bias-corrected) POLCOMS-ERSEM projections predicted reasonable values (i.e., consistent with historical observations) for the continental shelf around the Ebre delta and in the central part of the area, the projections of high chlorophyll-*a* concentrations for the northern part (north of approximately 41.50º N) seem unrealistically high. This has been identified as being due to the excessive riverine nutrient load modelled for the Rhône River (Ciavatta et al. 2019). The results of other modelling efforts (e.g., Macias et al. 2015) suggest that the western Mediterranean should become more oligotrophic in future decades due to increased stratification (strength and duration), and Kay et al. (2018) already recognize a positive bias of POLCOMS-ERSEM in chlorophyll-*a* projections. Our attempt to correct for bias in the northernmost part of our region with the help of observational data for the summers of 2011 and 2012 solved the problem for the 2010s projections but not for the 2050s or 2090s.

4.2 Potential spawning habitat

The potential spawning habitat of the anchovy, as indicated by the distribution of anchovy eggs, is projected to decrease importantly in the traditional spawning grounds of the Ebre River continental shelf. It is known that this area receives inflow of low saline and productive surface runoff waters, which offer favourable conditions for spawning and larval survival (Palomera et al. 2007; Sabatés et al. 2013). Therefore, it is to be expected that under the climate change scenarios examined here (RCP4.5 and 8.5), higher salinity and lower productivity around the Ebre delta resulting from a decrease in runoff water inputs, will likely decrease the spawning habitat suitability of anchovy. Under both future scenarios, the abundance of larvae would be lower than at the present time, suggesting that even if conditions for spawning could be maintained in the future, larval habitat is likely to shrink. In this regard, during the successive heat waves affecting southwestern Europe in summer 2003 (Schär and Jendritzky 2004), which resulted in exceptionally high sea water temperatures, the abundance of anchovy eggs and larvae was much lower than during the years with non-extreme conditions (Maynou et al. 2014). In the northern part of the area, the low abundance of anchovy eggs and larvae projected by the model under both scenarios is initially surprising and points to the limitation of extrapolating SDM models ignoring dynamic processes. In our case, a projection model taking into account changes in the potential spawning habitat of anchovy in the Gulf of Lions and transport of larvae towards the south would provide a more realistic picture of the future distribution of anchovy larvae in the northernmost part of our study area. It must be considered that the high concentrations of anchovy larvae that have been regularly found in the northern area are due to, in addition to local production, their transport by the Northern Current, which flows southwards along the continental slope (Sabatés et al. 2007). These larvae are advected by the current from the northern spawning ground in the Gulf of Lions and aggregated by mesoscale anticyclonic eddies generated by instabilities in the current (Sabatés et al. 2007, 2013; Ospina-Álvarez et al. 2015). Hence, the above considerations suggest that the projected low abundance of anchovy larvae in the northernmost part of the area was not due to temperature, salinity or the (unbiased) chlorophyll-*a* values projected by the model but rather due to the absence in the model of larval transport due to currents and phenomena of mesoscale dynamics. Combining biogeochemical models with suitably calibrated larval transport models would help to clarify the importance of larval transport and connectivity between spawning and recruitment locations (Lacroix et al. 2018). The number of larvae advected to a given area results from the complex interaction between temperature, current direction and speed, and the trophic resources in the dynamic environment surrounding larvae. In simulation models of climatic change, the net result appears highly variable and species-specific, with some studies predicting increased larval duration and reduced recruitment success (Lacroix et al. 2018), while other research results highlight the role of larval retention for successful recruitment and population persistence (Patti et al. 2020).

In the case of round sardinella, the probability of encountering eggs or larvae is projected to increase under both scenarios, and more so under RCP8.5 conditions. The effect was more noticeable for larvae than for eggs. This trend was related to the temperature increase favouring this thermophilic species (Sabatés et al. 2006). Note, however, that under RCP4.5, the highest probability of encountering larvae was in the mid-century projection, while in RCP8.5, the probabilities were not significantly different between the mid and the late 21st century. It is likely that an increase in salinity combined with decreasing primary productivity will decrease the northward expansion of this species, which has strictly coastal spawning grounds. In any case, our modelling results were consistent with the increasing presence and abundance of round sardinella (a tropical to subtropical species that is distributed globally) in the area, linked with progressive sea water warming (Palomera et al. 2007; Sabatés et al. 2009; Maynou et al. 2014; van Beveren et al. 2016).

4.3 Study limitations and future prospects

The modelling results presented here show a high degree of uncertainty because they attempt to capture only the statistical relationship between the surface water conditions and the abundance or presence of early life stages of fish. The surface variables considered have been proven to be good descriptors of the spawning habitat and larval environment of both species in the area (Palomera et al. 2007; Sabatés et al. 2013; Maynou et al. 2014). Coupling our spatial distribution model derived from present-day conditions into the future environmental conditions projected by the POLCOMS-ERSEM biogeochemical model can only provide an estimate of the average values of the potential fish habitat, without adequately considering the transient climatic phenomena or mid- to low-frequency forcing by climatic oscillations, such as the NAO or the AMO, which are known to significantly affect the climate of European waters (Alexander et al. 2018). Other important factors determining the spatial distribution (both horizontal and vertical) of fish eggs and larvae, such as mesoscale phenomena or the vertical structure of the water mass (Bakun 2006; Olivar et al. 2010; Ospina-Álvarez et al. 2015), could not be incorporated into the analysis due to the lack of synoptic data, but as mentioned before, larval transport and mesoscale dynamics have been shown to be important factors in explaining the spatial distribution of early anchovy life stages. Future developments in this field would require the incorporation of dynamic models to predict the spatial distribution of fishes, with the caveats and difficulties already identified by Checkley et al. (2017).

In our modelling approach, the values of the environmental variables were taken as accurate, with no consideration of the possible uncertainty associated with the estimation of these variables in the biogeochemical model(s). Naturally, incorporating biogeochemical model uncertainty and structural uncertainty into the spatial distribution model would amplify the variability in the estimations (Payne

et al. 2016). To this end, there is a need to create i) large calibration datasets for biogeochemical models in the Mediterranean by gathering *in situ* observations that help validate the performance and skills of coupled biogeochemical models in three dimensions and through time, and ii) ensemble models for the Mediterranean; that is, making available to the research community a set of comparable models aiming to capture the same oceanographic processes.

More accurate and precise projections of the spatial distribution of marine fishes will be obtained by considering mechanistic/physiological, or density-dependent effects, among other factors (Checkley et al. 2017), but we should not forget that past or current conditions may not repeat in the future ("non-ergodicity" and other limits to predictability; Planque 2016). Other aspects, such as changes in the phenology of spawning linked to both temperature and plankton production, are expected and are typically estimated on the order of a shift of 1-2 weeks under RCP8.5 by the end of the century (e.g., Asch et al., 2019). Given the protracted spawning season of these species, changes in phenology would probably not affect our main projections of changes in the suitability of the spawning area during the June-July months used in the model. However, we cannot overlook the potential effects of prolonged heat waves or other extreme weather anomalies (Schär and Jendritzky 2004), which could have a more pronounced impact on the interannual variability of the reproductive success of these species.

Acknowledgements

This work has received funding from the European Union's Horizon 2020 research and innovation programme under the Grant Agreement "CERES" No. 678193 and from the Spanish Ministry of Economy and Competitiveness (CTM2010-18874 and CTM2015-68543-R). Eduardo Ramirez-Romero is thankful for the funding from "Govern de les Illes Balears—Conselleria d'Innovació, Recerca i Turisme, Programa Vicenç Mut."

5 References

Alexander MA, Scott JD, Friedland KD et al (2018) Projected sea surface temperatures over the 21st century: Changes in the mean, variability and extremes for large marine ecosystem regions of Northern Oceans. Elem Sci Anth 6(1): 9. DOI: https://doi.org/10.1525/elementa.191

Asch RG, Stock CA, Sarmiento JL (2019) Climate change impacts on mismatches between phytoplankton blooms and fish spawning phenology. Glob Change Biol 25: 2544-2559. DOI: https://doi.org/10.1111/gcb.14650

Azzurro E, Moschella P, Maynou F (2011) Tracking Signals of Change in Mediterranean Fish Diversity Based on Local Ecological Knowledge. PLoS ONE 6(9): e24885. DOI : https://doi.org/10.1371/journal.pone.0024885

Bakun A (2006) Fronts and eddies as key structures in the habitat of marine fish larvae: opportunity, adaptive response and competitive advantage. Sci Mar 70(S2): 105-122

Brosset P, Menard F, Fromentin J, Bonhommeau S, Ulses C, Bourdeix J, Bigot J, et al (2015). Influence of environmental variability and age on the body condition of small pelagic fish in the Gulf of Lions. Mar Ecol Prog Ser 529: 219–231. DOI: https://doi.org/10.3354/meps11275

Brown CJ, Schoeman DS, Sydeman WJ, Brander K, Buckley LB, Burrows M, Duarte CM, Moore PJ, Pandolfi JM, Poloczanska E, Venables W, Richardson AJ (2011) Quantitative approaches in climate change ecology. Glob Chang Biol 17:3697–3713. DOI: https://doi.org/10.1111/j.1365-2486.2011.02531.x

Butenschön M, Clark J, Aldridge JN, Allen JI, Artioli Y, Blackford J, Bruggeman J, Cazenave P, Ciavatta S, Kay S, Lessin G, van Leeuwen S, van der Molen J, de Mora L, Polimene L, Sailley S, Stephens N, Torres R (2016) ERSEM 15.06: a generic model for marine biogeochemistry and the ecosystem dynamics of the lower trophic levels. Geosci. Model Dev. 9: 1293–1339. DOI: https://doi.org/10.5194/gmd-9-1293-2016

Catalán IA, Auch D, Kamermans P, Morales-Nin B, Angelopoulos NV, Reglero P, Sandersfeld T, Peck MA (2019) Critically examining the knowledge base required to mechanistically project climate impacts: A case study of Europe's fish and shellfish. Fish Fish 20(3): 501-517. DOI: https://doi.org/10.1111/faf.12359

Checkley DM Jr, Alheit J, Oozeki Y, Roy C (2009) Climate Change and Small Pelagic Fish. Cambridge University Press, Cambridge, 372 pp.

Checkley DM Jr, Asch RG, Rykaczewski RR (2017) Climate, Anchovy, and Sardine. Annu Rev Mar Sci 9: 469-493. DOI: https://doi.org/10.1146/annurev-marine-122414-033819

Ciavatta S, Kay S, Brewin RJW, Cox R, Di Cicco A, Nencioli F, Polimene L, Sammartino M, Santoleri R, Skákala J, Tsapakis M (2019) Ecoregions in the Mediterranean Sea through the reanalysis of phytoplankton functional types and carbon fluxes. J Geophys Res Ocean (in press) DOI: https://doi.org/10.1029/2019JC015128

CIESM (2008) Climate Warming and Related Changes in Mediterranean Marine Biota. CIESM Workshop Monographs, 35. Monaco. 152 pp.

Colella S, Falcini F, Rinaldi E, Sammartino M, Santoleri R (2016) Mediterranean Ocean Colour Chlorophyll Trends. PLoS ONE 11(6): e0155756. DOI: https://10.1371/journal.pone.0155756

Coll M, Albo-Puigserver M, Navarro J, Palomera I, Dambacher J M (2018) Who is to blame? Plausible pressures on small pelagic fish population changes in the northwestern Mediterranean Sea. Mar. Ecol. Prog. Ser. 617-618: 277-294. DOI: https ://doi.org/10.3354/meps1 2591

Coma R, Ribes M, Serrano E, Jiménez E, Salat J, Pascual J (2009) Global warming-enhanced stratification and mass mortality events in the Mediterranean. Proc Nat Acad Sci USA 106(15): 6176-6181. DOI: https://doi.org/10.1073/pnas.0805801106

Dulvy NK, Rogers SI, Jennings S, Stetzenmüller V, Dye SR, Skjoldal HR (2008) Climate change and deepening of the North Sea fish assemblage: a biotic indicator of warming seas. J Appl Ecol 45: 1029-1039

Durrieu de Madron X et al (2011) Marine ecosystems' responses to climatic and anthropogenic forcings in the Mediterranean. Prog Oceanogr 91: 97-166

Elith J, Leathwick JR (2009) Species distribution models: ecological explanation and prediction across space and time. Annu Rev Ecol Evol Syst 40: 677–697

Erauskin-Extramiana M, Alvarez P, Arrizabalaga H, Ibaibarriaga L, Uriarte A, Cotano U, Santos M, Ferrer L, Cabré A, Irigoien X, Chust G (2019) Historical trends and future distribution of anchovy spawning in the Bay of Biscay. Deep Sea Res Part II Top Stud Oceanogr 159: 169–182. DOI: https://doi.org/10.1016/j.dsr2.2018.07.007

Estrada M (1996) Primary production in the northwestern Mediterranean. Sci Mar 60:55–64

Estrada M, Marrasé C, Latasa M, Berdalet E, Delgado M, Riera T (1993) Variability of deep chorophyll maximum characteristics in the Northwestern Mediterranean. Mar Ecol Prog Ser 92: 289–300

Font J, Salat J, Tintoré J (1988) Permanent features of the circulation in the Catalan sea. In: Minas HJ, Nival P (eds) Pelagic Mediterranean oceanography. Oceanol Acta 9: 51–57

Giannoulaki M, Iglesias M, Tugores MP, Bonanno A, Patti B, et al (2013) Characterizing the potential habitat of European anchovy *Engraulis encrasicolus* in the Mediterranean sea, at different life stages. Fish Oceanog 22(2): 68-89

Guisan A, Thuiller W (2005) Predicting species distribution: offering more than simple habitat models. Ecol Lett 8: 993–1009

Guisan A, Zimmermann NE (2000) Predictive habitat distribution models in ecology. Ecol Model 135: 147–186

Gudmundsson L, Bremnes JB, Haugen JE, Engen-Skaugen T (2012) Technical Note: Downscaling RCM precipitation to the station scale using statistical transformations -- A comparison of methods. Hydrol Earth Syst Sci 16: 3383–3390. DOI: https://doi.org/10.5194/hess-16-3383-2012

Halpern BS, Walbridge S, Selkoe KA et al (2008) A global map of human impact on marine ecosystems. Science 319(5865): 948-953. DOI: https//doi.org/ 10.1126/science.1149345

Hiddink JG, Burrows MT, Molinos JG (2015) Temperature tracking by North Sea benthic invertebrates in response to climate change. Glob. Change Biol. 21, 117-129. DOI: https://doi.org/10.1111/gcb.12726

Hirzel AH, Le Lay G, Helfer V, Randin C, Guisan A (2006) Evaluating the ability of habitat suitability models to predict species presences. Ecol. Model. 199: 142–152

Holt JT, James ID, Jones JE (2001) An s coordinate density evolving model of the northwest European continental shelf 1, Model description and density structure. J Geophys Res 106: 14015-14034. DOI: https://doi.org/10.1029/2000JC000304

Holt J, Wakelin S, Lowe J, Tinker J (2010) The potential impacts of climate change on the hydrography of the northwest European continental shelf. Prog Oceanogr 86(3-4): 361-379. DOI: https://doi.org/ 10.1016/j.pocean.2010.05.003

Holt J, Butenschön M, Wakelin SL, Artioli Y, Allen JI (2012) Oceanic controls on the primary production of the northwest European continental shelf: model experiments under recent past conditions and a potential future scenario. Biogeosciences 9: 97–117. DOI: https://doi.org/10.5194/bg-9-97-2012

Iona A, Theodorou A, Sofianos S, Sylvain W, Troupin C, Beckers J-M (2018) Mediterranean Sea climatic indices: monitoring long-term variability and climate changes. Earth Syst Sci Data 10: 1829–1842. DOI: https://doi.org/10.5194/essd-10-1829-2018

Kay S, Butenschön M (2018) Projections of change in key ecosystem indicators for planning and management of marine protected areas: An example study for European seas. Est. Coast Shelf Sci. 201: 172-184. DOI: https://10.1016/j.ecss.2016.03.003

Kay S, Andersson H, Catalan I, Eilola K, Jordà G, Ramirez-Romero E, Wehde W (2018) Projections of physical and biogeochemical parameters and habitat indicators for European seas, including synthesis of Sea Level Rise and storminess. H2020 CERES project deliverable D1.3, https://ceresproject.eu/

Lacroix G, Barbut L, Volckaert FAM (2018) Complex effect of projected sea temperature and wind change on flatfish dispersal. Global. Change Biol. 24(1): 85-100.

Macias D, Garcia-Gorriz E, Stips A (2018) Productivity changes in the Mediterranean Sea for the twenty-first century in response to changes in the regional atmospheric forcing. Front Mar Sci 16, 76. https://doi.org/10.3389/fmars.2015.00079

Macias D, Garcia-Gorriz E, Stips A (2018) Deep winter convection and phytoplankton dynamics in the NW Mediterranean Sea under present climate and future (horizon 2030) scenarios. Sci Rep 8, 1–15.

Martín P, Sabatés A, Lloret J, Martin-Vide J (2012) Climate modulation of fish populations: the role of the Western Mediterranean Oscillation (WeMO) in sardine (*Sardina pilchardus*) and anchovy (*Engraulis encrasicolus*) production in the north-western Mediterranean. Clim Change 110: 925-939. DOI: https://doi.org/10.1007/s10584-011-0091-z

Maynou F (2014) Co-viability analysis of Western Mediterranean fisheries under MSY scenarios for 2020. ICES J Mar Sci 71(7): 1563 – 1571. DOI: https://doi.org/10.1093/icesjms/fsu061

Maynou F, Sabatés A, Salat J (2014) Clues from the recent past to assess recruitment of Mediterranean small pelagic fishes under sea warming scenarios. Clim Change 126(1-2): 175-188. DOI: https://doi.org/10.1007/s10584-014-1194-0

Maynou F, Sabatés A, Raya V (2020) Changes in the spawning habitat of two small pelagic fish in the Northwestern Mediterranean. Fish Oceanogr DOI: 10.1111/fog.12464

Nevárez-Martínez MO, Lluch-Belda D, Cisneros-Mata MA, Santos-Molina JP, Martínez-Zavala MDLA, Lluch-Cota SE (2001) Distribution and abundance of the Pacific sardine (*Sardinops sagax*) in the Gulf of California and their relation with the environment. Prog Oceanogr 49:565–580.

Millot, C (1999) Circulation in the western Mediterranean Sea. J Mar Syst 20: 423–442.

Olivar, MP, Salat, J, Palomera, I (2001) Comparative study of spatial distribution patterns of the early stages of anchovy and pilchard in the NW Mediterranean Sea. Mar Ecol Prog Ser 217: 111–120.

Olivar MP, Emelianov M, Villate F, Morote E (2010) The role of oceanographic conditions and plankton availability in larval fish assemblages off the Catalan coast (NW

Mediterranean). Fish Oceanogr 19(3): 209 – 229. DOI: https://doi.org/10.1111/j.1365-2419.2010.00538.x

Ospina-Alvarez A, Catalán IA, Bernal M, Roos D, Palomera I (2015) From egg production to recruits: Connectivity and inter-annual variability in the recruitment patterns of European anchovy in the northwestern Mediterranean. Prog Oceanogr 138: 431–447. DOI: https://doi.org/ 10.1016/j.pocean.2015.01.011

Palomera I, Olivar MP, Salat J, Sabatés A, Coll M, García A, Morales-Nin B (2007) Small pelagic fish in the NW Mediterranean sea: an ecological review. Prog Oceanogr 74: 377–396. DOI: https://doi.org/10.1016/j.pocean.2007.04.012

Pastor F, Valiente JA, Palau JL (2018) Sea Surface Temperature in the Mediterranean: Trends and Spatial Patterns (1982–2016) Pure Appl. Geophys. (2018) 175: 4017. DOI: https://doi.org/10.1007/s00024-017-1739-z

Payne MR, Barange M, Cheung WWL, MacKenzie BR, Batchelder HP, et al. (2016) Uncertainties in projecting climate-change impacts in marine ecosystems. ICES J Mar Sci 73(5): 1272-1282

Peck MA Arvanitidis C, Butenschön M, Canu DM, Chatzinikolaou E et al (2018) Projecting changes in the distribution and productivity of living marine resources: A critical review of the suite of modelling approaches used in the large European project VECTORS. Est Coast Shelf Sci 201: 40-55. DOI: https://10.1016/j.ecss.2016.05.019

Planque B, Bellier E, Lazure P (2007) Modelling potential spawning habitat of sardine (*Sardina pilchardus*) and anchovy (*Engraulis encrasicolus*) in the Bay of Biscay. Fish Oceanogr 16:16–30

Planque B, Loots C, Petitgas P, Lindström U, Vaz S (2011) Understanding what controls the spatial distribution of fish populations using a multi-model approach. Fish Oceanogr 20(1): 1-17. DOI: https://doi.org/10.1111/j.1365-2419.2010.00546.x

Planque B (2016) Projecting the future state of marine ecosystems, “la grande illusion”? ICES J Mar Sci 73: 204–208. DOI: https://doi.org/10.1093/icesjms/fsv155

Sabatés A, Martín P, Lloret J, Raya V (2006) Sea warming and fish distribution: the case of the small pelagic fish, *Sardinella aurita*, in the western Mediterranean. Glob Change Biol 12: 2209–2219

Sabatés A, Salat J, Palomera I, Emelianov, M., De Puelles MLF, Olivar MP (2007) Advection of anchovy (*Engraulis encrasicolus*) larvae along the Catalan continental slope (NW Mediterranean). Fish Oceanogr 16(2): 130-141. DOI: https://doi.org/ 10.1111/j.1365-2419.2006.00416.x

Sabatés A, Salat J, Raya V, Emelianov M, Segura-Noguera M (2009) Spawning environmental conditions of *Sardinella aurita* at the northern limit of its distribution range, the western Mediterranean. Mar Ecol Prog Ser 385: 227–236. DOI: https://doi.org/10.3354/meps08058

Sabatés A, Salat J, Raya V, Emelianov M (2013) Role of mesoscale eddies in shaping the spatial distribution of the coexisting *Engraulis encrasicolus* and *Sardinella aurita* larvae in the northwestern Mediterranean. J Mar Syst 111: 108–119. DOI: https://doi.org/ 10.1016/j.jmarsys.2012.10.002

Sabatés A, Salat J, Tilves U, Raya V, Purcell JE, Pascual M, Gili JM, Fuentes VL (2018) Pathways for *Pelagia noctiluca* jellyfish intrusions onto the Catalan shelf and their interactions with early life fish stages. Journal of Marine Systems 187: 52-61. DOI: https://doi.org/ 10.1016/j.jmarsys.2018.06.013

Salat J (1996) Review of hydrographic environmental factors that may influence anchovy habitats in northwestern Mediterranean. Sci Mar 60(2):21–32

Salat J, García MA, Cruzado A, Palanques A, Arín L, Gomis D, Guillén J, de León A, Puigdefàbregas J, Sospedra J, Velásquez ZR (2002) Seasonal changes of water mass structure and shelf slope exchanges at the Ebro shelf (NW Mediterranean). Cont Shelf Res 22:327–346

Schär C, Jendritzky G (2004) Climate change: hot news from summer 2003. Nature 432, 559–560.

Siokou-Frangou I, Christaki U, Mazzocchi MG, Montresor M, Ribera d'Alcalá M, Vaqué D, Zingone A (2010) Plankton in the open Mediterranean Sea: a review. Biogeosciences 7: 1543–1586. DOI: https://doi.org/10.5194/bg-7-1543-2010

Taboada FG, Anadón R (2016) Determining the causes behind the collapse of a small pelagic fishery using Bayesian population modelling. Ecol Appl 26(3): 886-898. DOI: http://doi.org/10.1890/15-0006

Van Beveren E, Fromentin J-M, Rouyer T, Bonhommeau S, Brosset P, Saraux C (2016) The fisheries history of small pelagics in the Northern Mediterranean. ICES J Mar Sci 73(6) : 1474-1485. DOI : https://doi.org/ 10.1093/icesjms/fsw023

TABLES

Table 1. Estimated non-parametric coefficients of GAM models relating environmental variables to the abundance of anchovy or presence of round sardinella early life stages (from Maynou et al. 2020.). SSS: sea surface salinity; Chl 20 m: Chlorophyll-a at 20 m depth, proxy for surface chlorophyll-a, SST: sea surface temperature. SE: Standard Error of coefficient; EDF: Estimated degrees of freedom.

Anchovy eggs	**Quasi-Poisson**	**Link=log**
Intercept	7.402 (SE 0.220)	p(t) <0.001
s(SSS)	3.963 (EDF 3.999)	p(F)<0.001
s(log Chl 20 m)	3.573 (EDF 3.897)	p(F)=0.052
s(SST)	2.360 (EDF 2.907)	p(F)=0.028
Anchovy larvae	**Quasi-Poisson**	**Link=log**
Intercept	7.653 (SE 0.150)	p(t) <0.001
s(log Chl 20 m)	3.169 (EDF 3.672)	p(F) <0.001
s(SSS)	3.814 (EDF 3.976)	p(F) <0.001
s(SST)	2.611 (EDF 3.163)	p(F) <0.015
Round sardinella eggs	**binomial**	**Link=logit**
Intercept	-5.315 (SE 0.705)	p(t) <0.001
s(log Chl 20 m)	1.000 (EDF 1.000)	p(F) <0.001
s(SST)	3.713 (EDF 3.941)	p(F) <0.001
s(SSS)	1.000 (EDF 1.000)	p(F) <0.001
Round sardinella larvae	**binomial**	**Link=logit**
Intercept	-6.178 (SE 1.143)	p(t) <0.001
s(SSS)	1.984 (EDF 2.449)	p(F) <0.001
s(SST)	1.880 (EDF 2.347)	p(F) <0.001

FIGURES

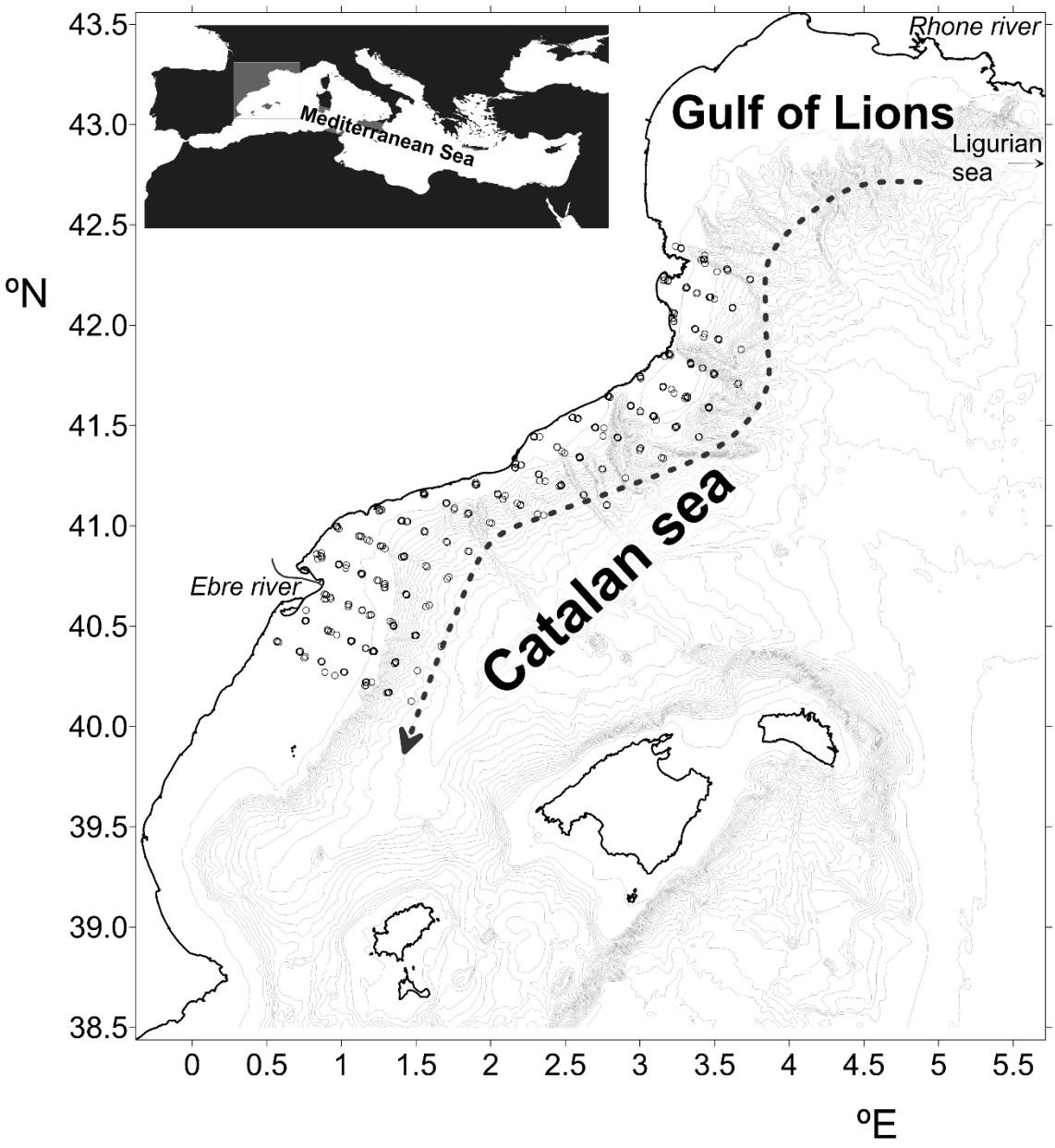

Fig. 1. Study area. The map shows the location of the ichthyoplankton surveys used to estimate the potential spawning habitat and depth contours at 100 m intervals (grey). The dotted line represents the typical path of the Northern Current.

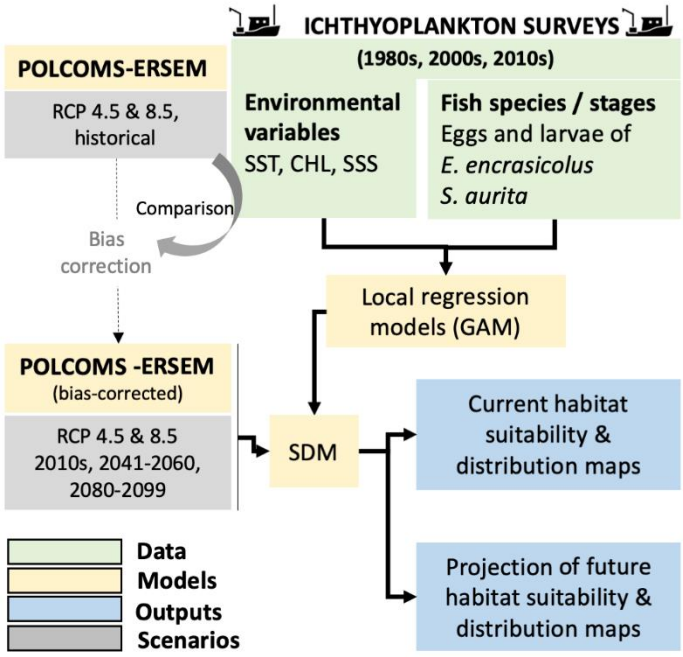

Fig. 2. Procedure to derive the spatial distribution models (SDM) of early life stages of anchovy (*Engraulis encrasicolus*) and round sardinella (*Sardinella aurita*) from ichthyoplankton surveys, local regression models (GAM) and projections based on future climate change scenarios (IPCC scenarios). The procedure to correct the biases of the biogeochemical model is indicated (see methods).

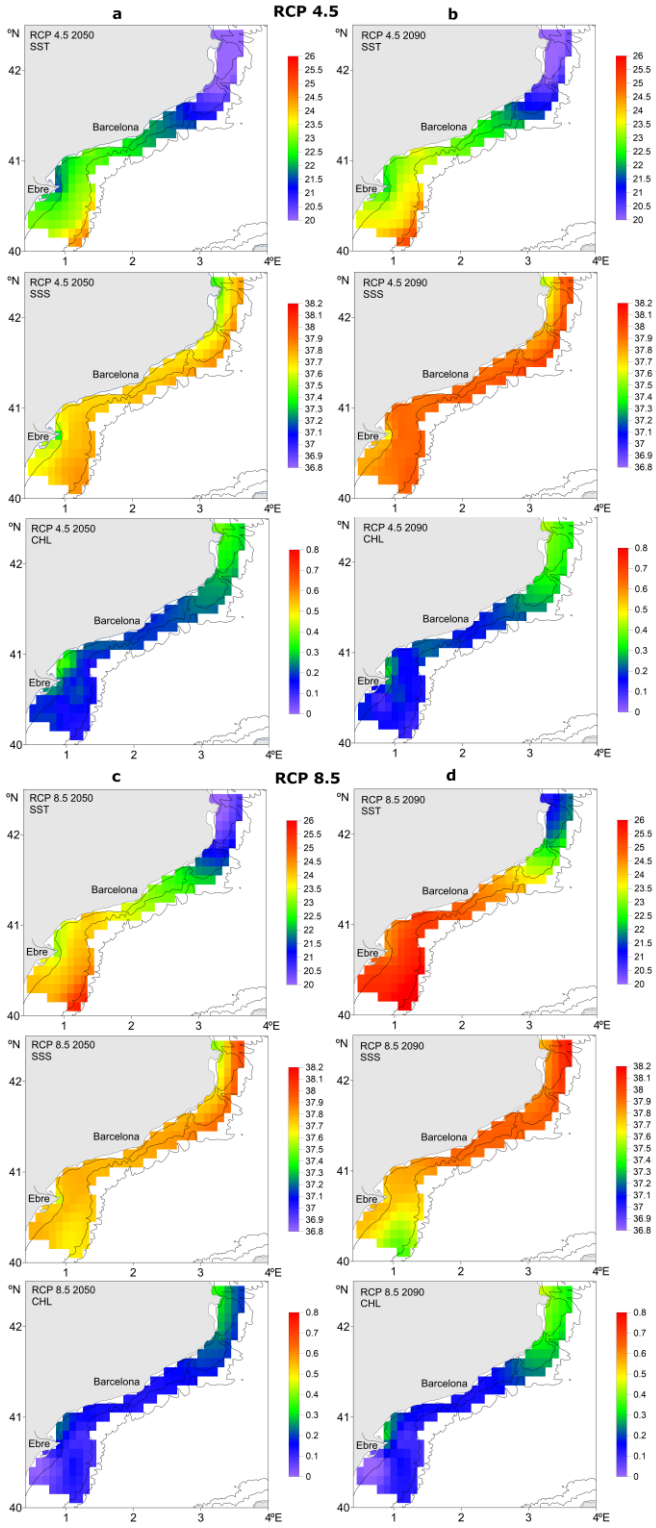

Fig. 3. Bias-corrected projections of environmental conditions (SST: Sea Surface Temperature, SSS: Sea Surface Salinity, CHL: Chlorophyll-*a*) under scenarios RCP4.5 [a, b] and RCP8.5 [c, d] for the decades 2041-2060 (2050s) and 2080-2099 (2090s).

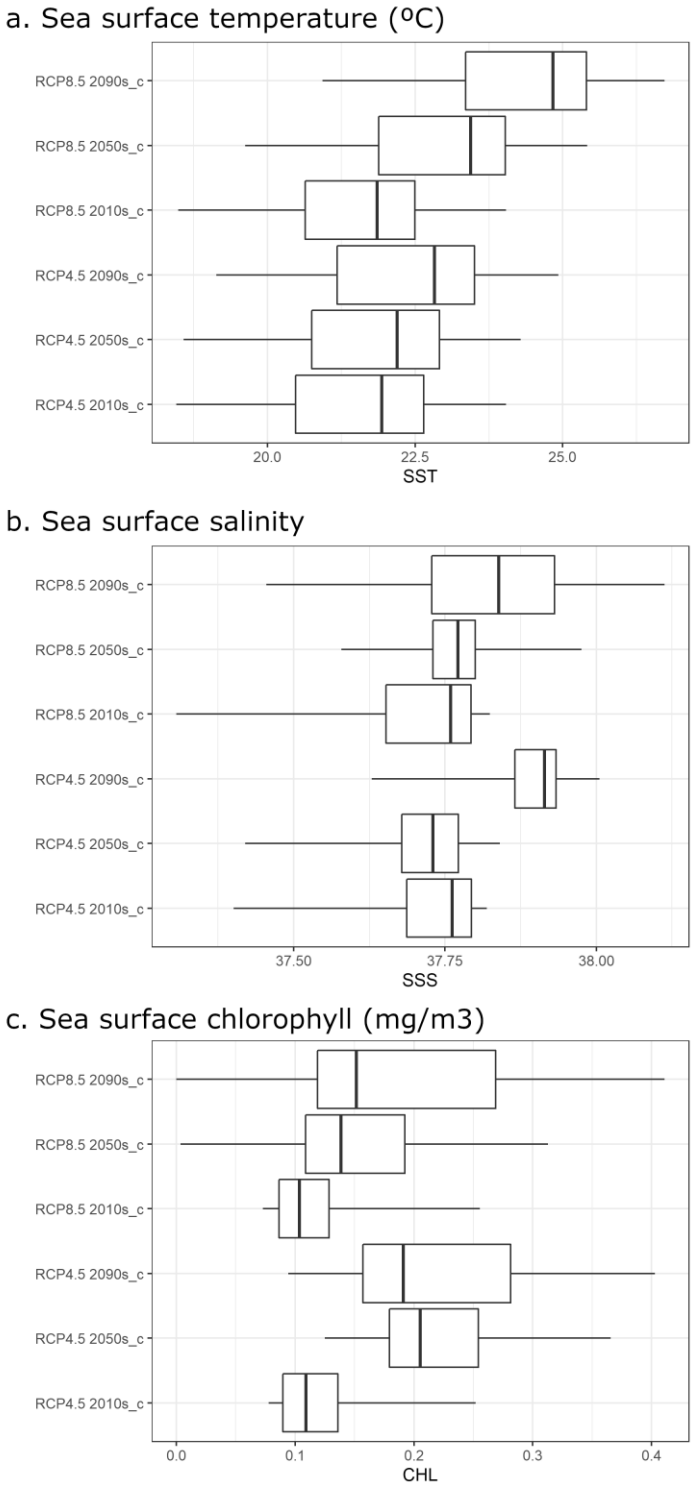

Fig. 4. Boxplots with 0.25, 0.50 (median) and 0.75 quantiles of the distribution of values of environmental variables forecast in the study area. Whiskers represent the minimum and maximum values forecast. All data are averages for the June and July months. Key: 2010s: model projection 2006-2015 data; 2050s and 2090s: forecast values for the middle (2041-2060) and final (2080-2099) decades of the 21st c.

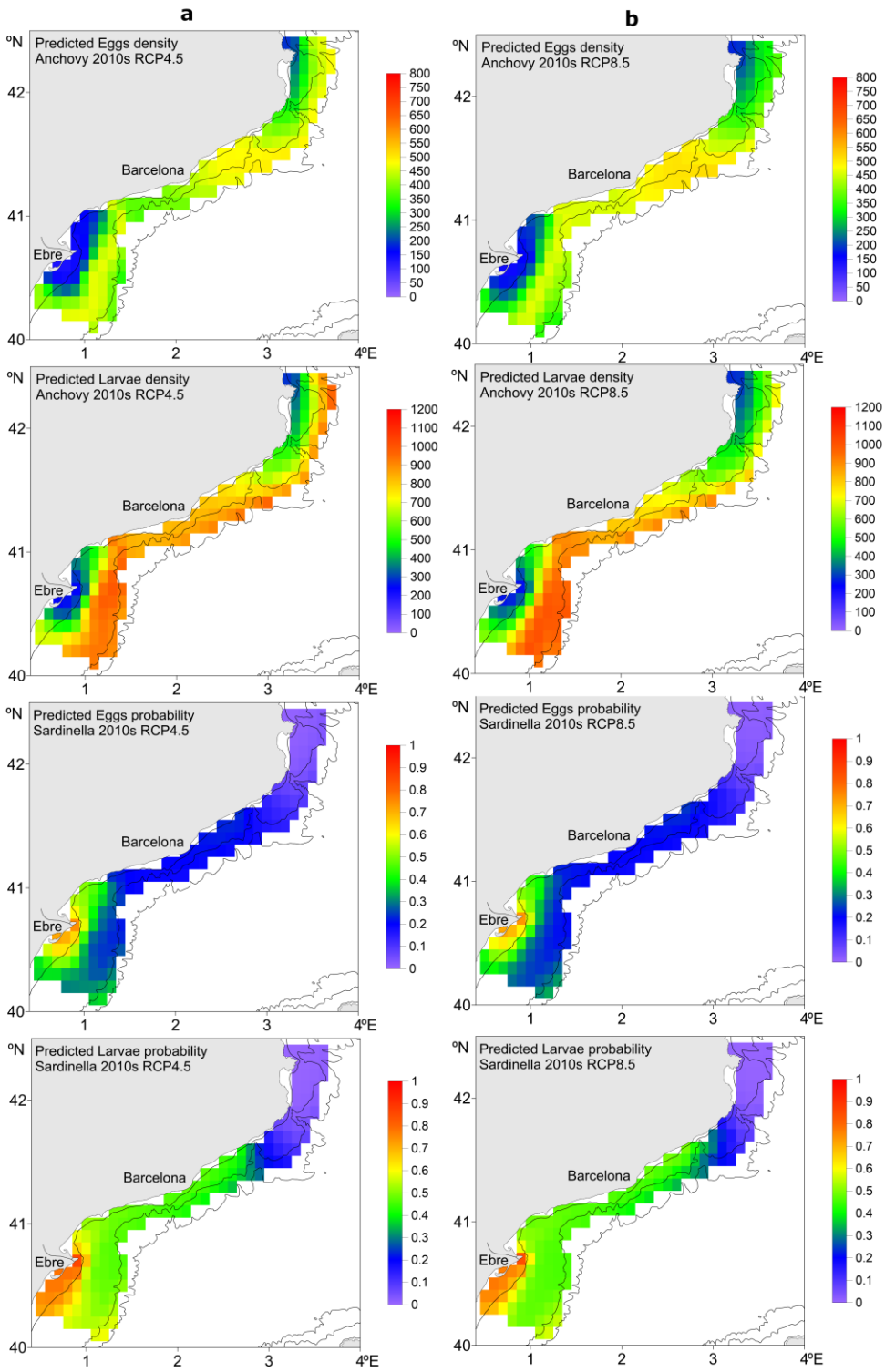

Fig. 5. Suitability maps for anchovy and round sardinella early life stages in the 2010s, computed by combining projected bias-corrected environmental variables (Electronic Supplemental Material, Annex 1) with the statistical spatial distribution models based on GAMs (Table 1).

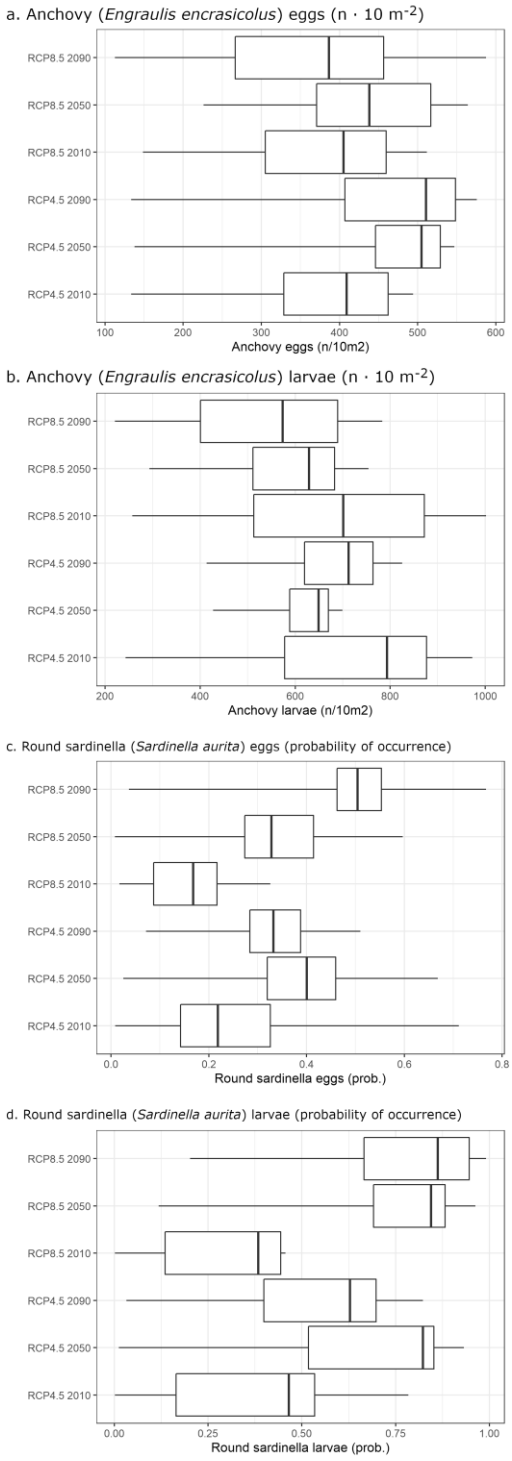

Fig. 6. Boxplots with 0.25, 0.50 (median) and 0.75 quantiles of the distribution of values of environmental variables projections in the study area. Whiskers represent the minimum and maximum values projections. All data are averages for the June and July months. 2010s; 2050s and 2090s: forecast values for the current (2006-2015), middle (2041-2060) and final (2080-2099) decades of the 21st c.

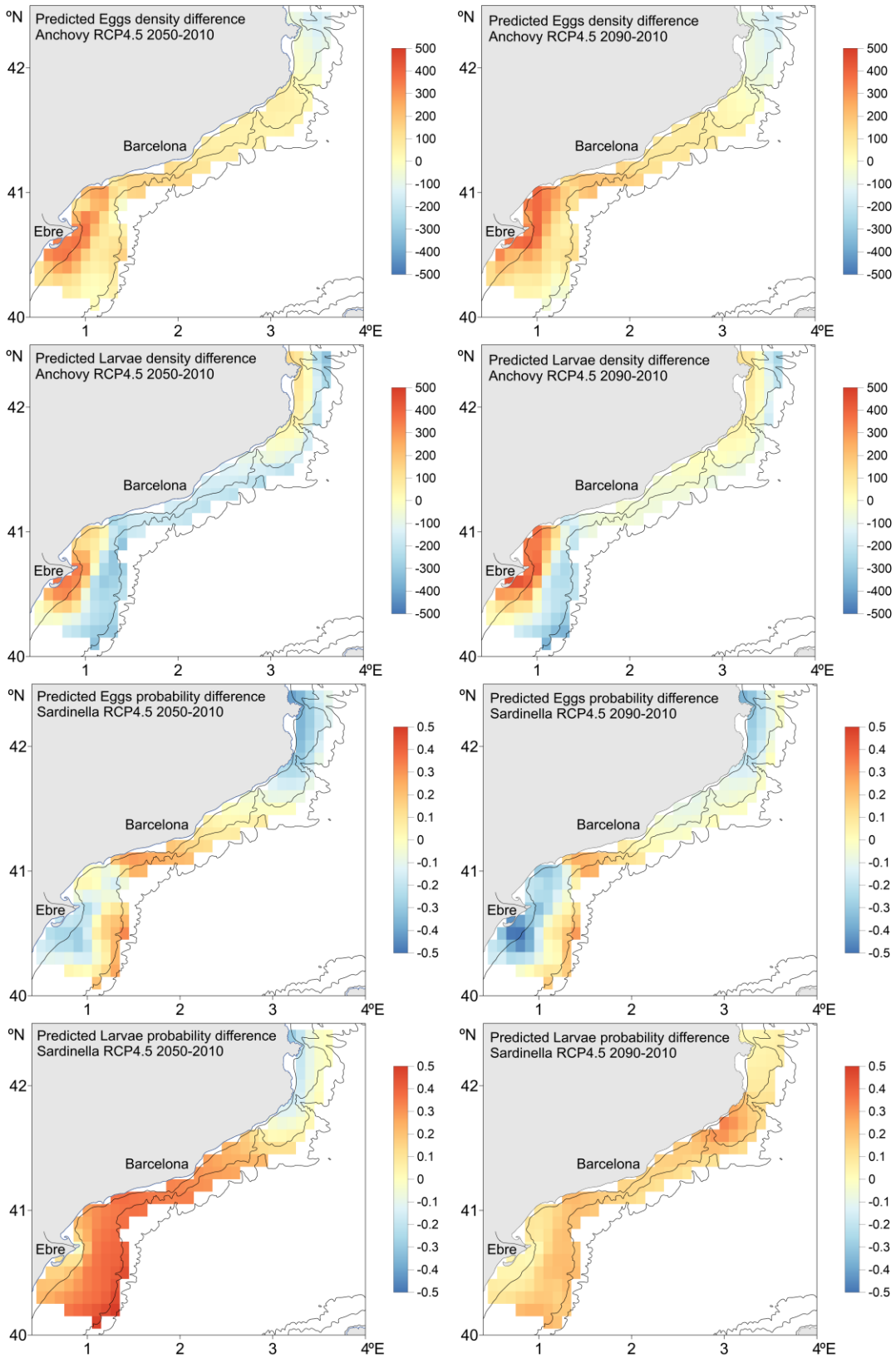

Fig. 7. Suitability difference map for anchovy (n · 10 m^{-2}) and round sardinella (probability of presence) early life stages under RCP4.5 between the mid or final decades of the 21st century and the 2010s.

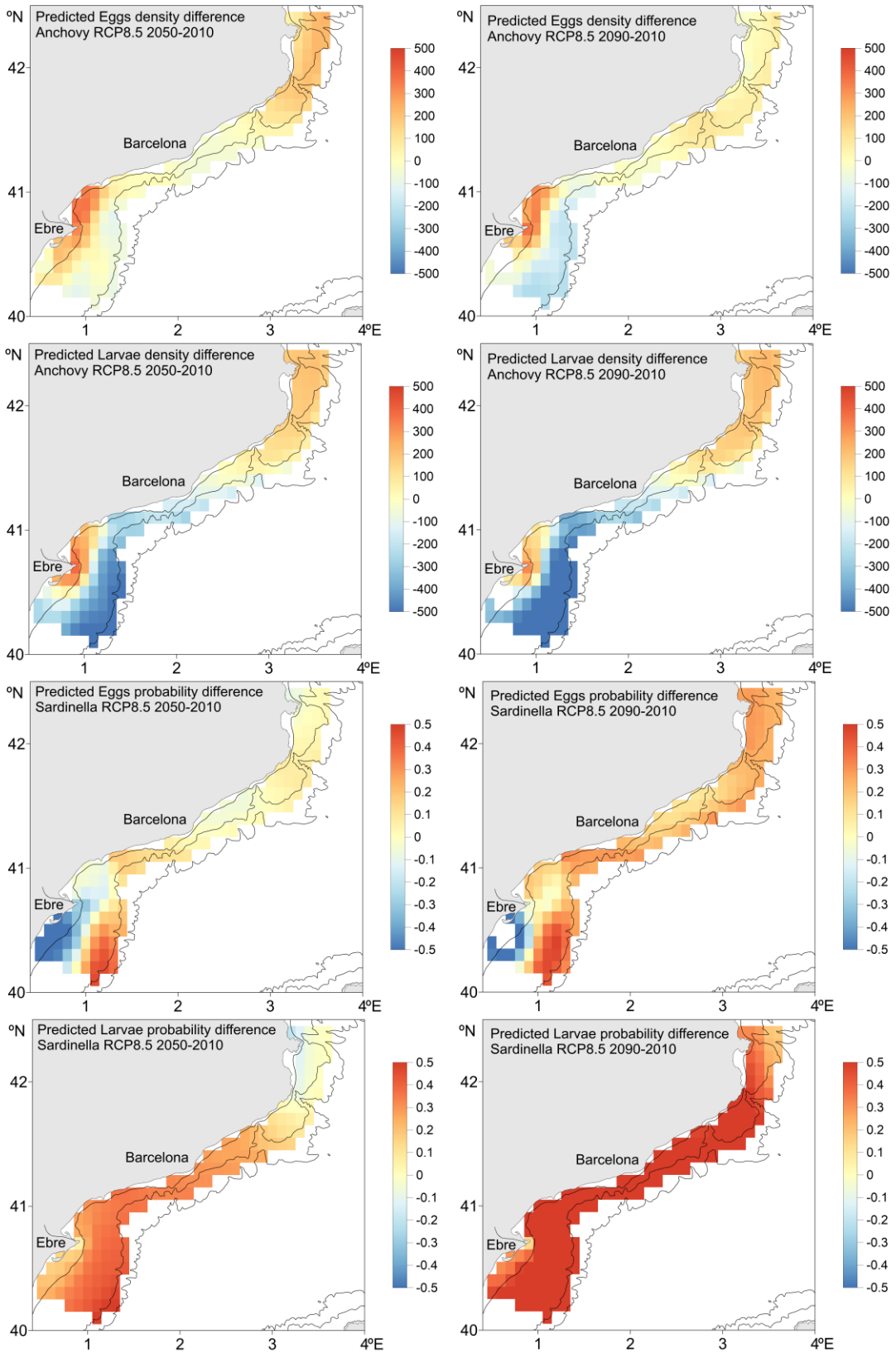

Fig. 8. Suitability maps (corrected for environmental bias) for the projected difference for anchovy (n · 10 m^{-2}) and round sardinella (probability of presence) early life stages under RCP8.5. between the mid or final decades of the 21st century and the 2010s.

Electronic Supplemental Material

Annex 1 – Environmental variables, current conditions (2006-2015).

Table S1. Estimated non-parametric coefficients of GAM models relating environmental variables to the abundance of anchovy or presence of round sardinella early life stages (from Maynou et al. 2020.). SSS: sea surface salinity; Chl 20 m: Chlorophyll-a at 20 m depth, proxy for surface chlorophyll-a, SST: sea surface temperature. SE: Standard Error of coefficient; EDF: Estimated degrees of freedom.

Anchovy eggs	**Quasi-Poisson**	**Link=log**
Intercept	7.402 (SE 0.220)	p(t) <0.001
s(SSS)	3.963 (EDF 3.999)	p(F)<0.001
s(log Chl 20 m)	3.573 (EDF 3.897)	p(F)=0.052
s(SST)	2.360 (EDF 2.907)	p(F)=0.028
Anchovy larvae	**Quasi-Poisson**	**Link=log**
Intercept	7.653 (SE 0.150)	p(t) <0.001
s(log Chl 20 m)	3.169 (EDF 3.672)	p(F) <0.001
s(SSS)	3.814 (EDF 3.976)	p(F) <0.001
s(SST)	2.611 (EDF 3.163)	p(F) <0.015
Round sardinella eggs	**binomial**	**Link=logit**
Intercept	-5.315 (SE 0.705)	p(t) <0.001
s(log Chl 20 m)	1.000 (EDF 1.000)	p(F) <0.001
s(SST)	3.713 (EDF 3.941)	p(F) <0.001
s(SSS)	1.000 (EDF 1.000)	p(F) <0.001
Round sardinella larvae	**binomial**	**Link=logit**
Intercept	-6.178 (SE 1.143)	p(t) <0.001
s(SSS)	1.984 (EDF 2.449)	p(F) <0.001
s(SST)	1.880 (EDF 2.347)	p(F) <0.001

POLCOMS-ERSEM (P.E.) average model estimates of SST, SSS, CHL for the period 2006-2015 (taken as representative of the 2010s decade) and estimates from CTD *in-situ* measurements ("observations") were compared to produce bias-corrected SST, SSS, CHL estimates for the 2010s decade. The bias correction was carried out using a quantile-linear transformation (Gudmundsson et al. 2012, R library *qmap*) with the observed CTD data for the 2010s from the "Fishjelly" cruises (2011 and 2012, Sabatés et al. 2018). Summary statistics for each data set are also provided.

RCP4.5 – SST

Model predictions (top, left) tended to yield higher temperatures than measured *in situ* (bottom left), particularly below 21.5° C. Conversely, model predictions yielded lower temperatures for temperature equal or higher than 23° C. Despite the bias, the overall trend in SST was well captured by the model.

Average summer SST predicted by P.E. model (uncorrected):

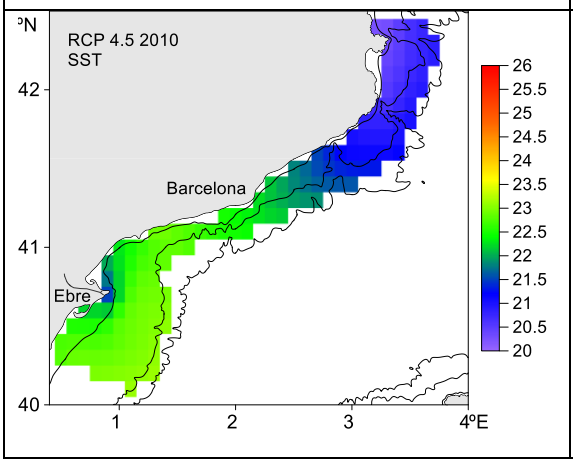

Average summer SST predicted by P.E. model (corrected or "de-biased"):

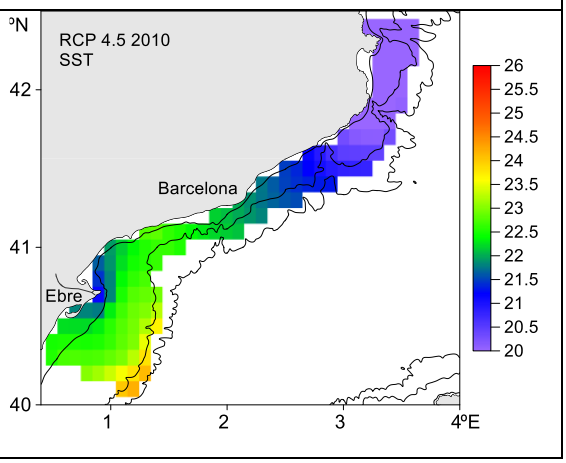

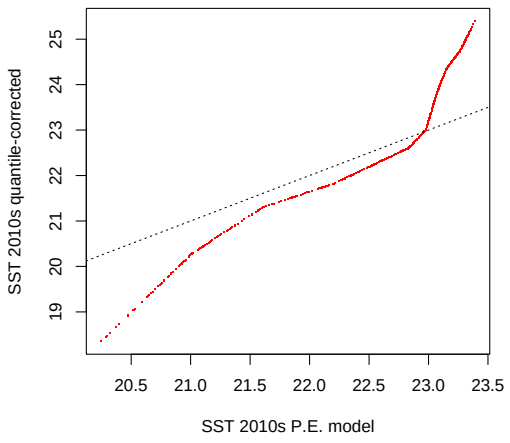

Quantiles of the 3 data sets:

P.E. model

```
Min. 1st Qu.  Median    Mean 3rd Qu.
Max.

20.25   21.99   22.84   22.48   23.10
23.39
```

Observed SST

```
Min. 1st Qu.  Median    Mean 3rd Qu.
Max.

18.46   21.52   22.59   22.65   24.11
25.33
```

quantile-corrected (qm.a)

```
Min. 1st Qu.  Median    Mean 3rd Qu.
Max.

18.35   21.63   22.62   22.64   24.00
25.40
```

RCP4.5 – SSS

Overall model predictions were positively biased, i.e. predicted salinity values (top left) were systematically higher than measured in the field (bottom left). The bias was particularly acute from 37.85 upwards. Despite the bias, the overall trend in SSS was well captured by the model.

Average summer SSS predicted by P.E. model (uncorrected):

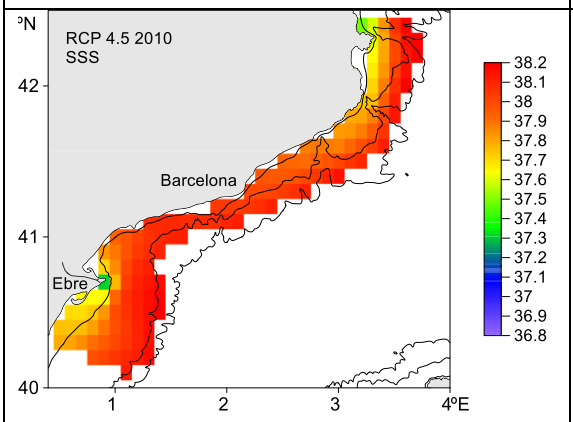

Average summer SSS predicted by P.E. model (corrected or "de-biased"):

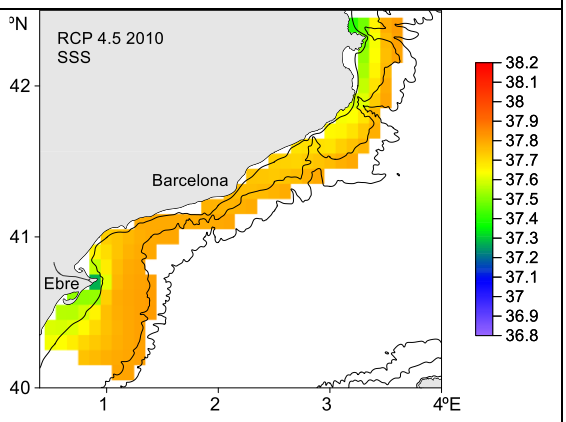

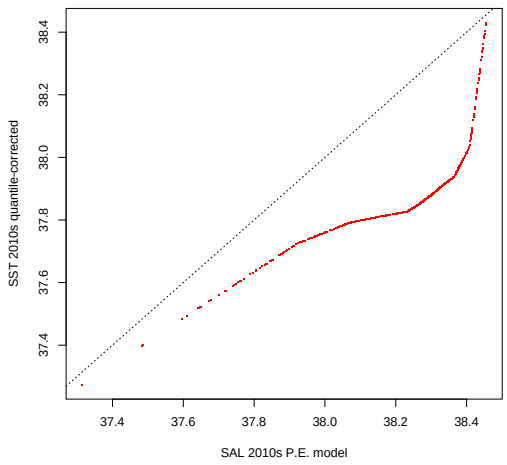

Quantiles of the 3 data sets:

```
P.E. model

Min. 1st Qu.  Median    Mean 3rd Qu.
Max.

37.31   38.12   38.27   38.21   38.35
38.46

Observed SSS

Min. 1st Qu.  Median    Mean 3rd Qu.
Max.

37.34   37.80   37.85   37.86   37.92
38.45

quantile-corrected (qm.a)

Min. 1st Qu.  Median    Mean 3rd Qu.
Max.

37.27   37.80   37.85   37.87   37.92
38.43
```

RCP 4.5 CHL

The model predictions of chlorophyll--*a* were positively biased overall (top left). The problem was particularly acute at 0.1 mg m^{-3} and higher (bottom left). Additionally, the model produced unrealistically high values of chlorophyll in the northern half of the area. The bias correction (right panel) successfully corrects this problem.

Average summer CHL predicted by P.E. model (uncorrected):

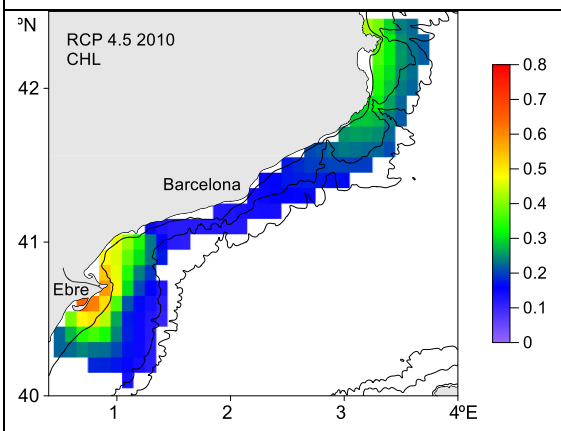

Average summer CHL predicted by P.E. model (corrected or “de-biased”):

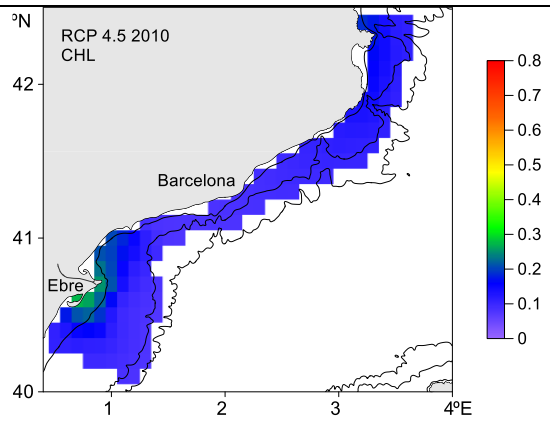

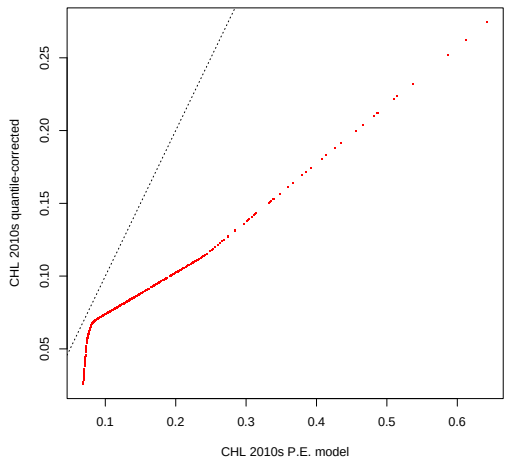

Quantiles of the 3 data sets:

P.E. model

```
Min. 1st Qu.  Median    Mean 3rd Qu.
Max.

0.0687 0.0791 0.1051 0.1420 0.1766
0.6424
```

Observed CHL

```
Min. 1st Qu.  Median    Mean 3rd Qu.
Max.

0.0294 0.0655 0.0753 0.0828 0.0979
0.2900
```

quantile-corrected (qm.a)

```
Min. 1st Qu.  Median    Mean 3rd Qu.
Max.

0.0258 0.0650 0.0754 0.0837 0.0956
0.2744
```

RCP8.5 – SST

same observations than for RCP4.5

Average summer SST predicted by P.E. model (uncorrected):	Average summer SST predicted by P.E. model (corrected or “de-biased”):
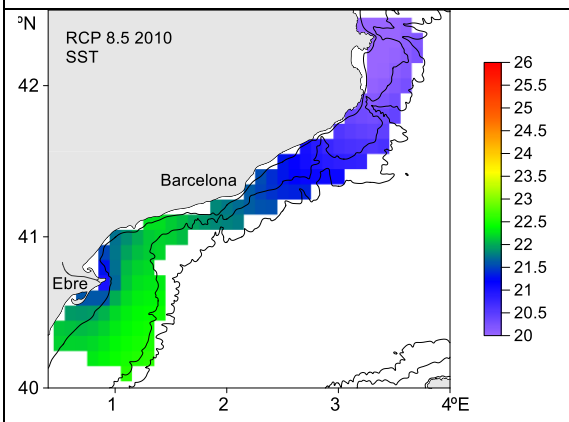	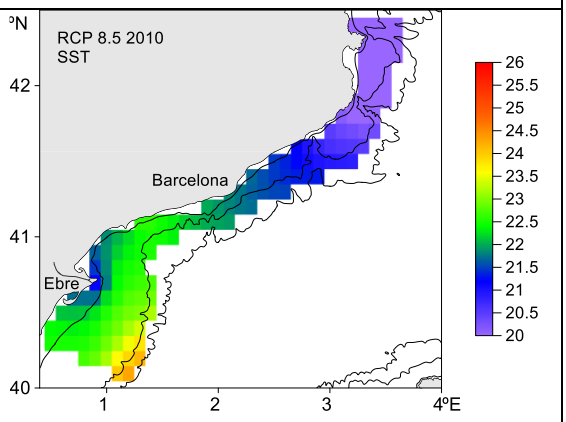

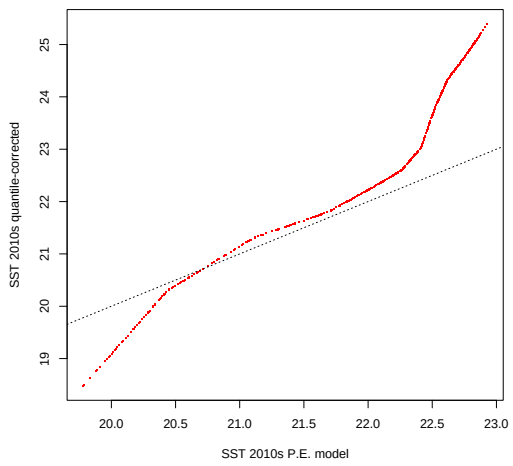

P.E. model

```
Min. 1st Qu.  Median    Mean 3rd Qu.
Max.

19.78   21.48   22.26   21.94   22.57
22.93
```

Observed SST

```
Min. 1st Qu.  Median    Mean 3rd Qu.
Max.

18.46   21.52   22.59   22.65   24.11
25.33
```

quantile-corrected (qm.a)

```
Min. 1st Qu.  Median    Mean 3rd Qu.
Max.

18.48   21.62   22.60   22.63   24.06
25.39
```

RCP8.5 – SSS

same observations than for RCP4.5

Average summer SSS predicted by P.E. model (uncorrected):	Average summer SSS predicted by P.E. model (corrected or “de-biased”):
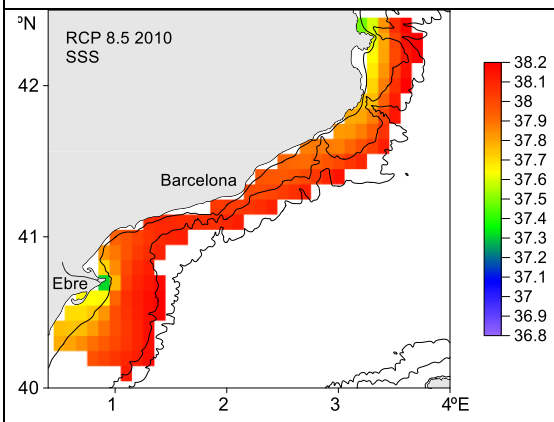	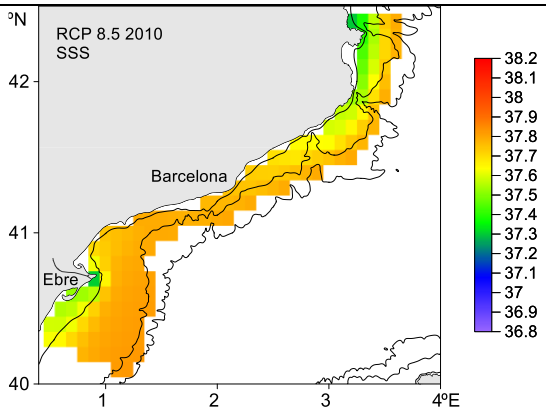

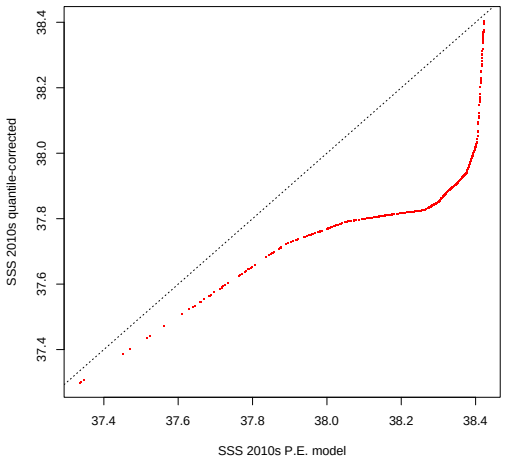

Quantiles of the 3 data sets:

P.E. model

```
Min. 1st Qu.  Median    Mean 3rd Qu.
Max.

37.34   38.11   38.30   38.22   38.36
38.42
```

Observed SSS

```
Min. 1st Qu.  Median    Mean 3rd Qu.
Max.

  37.34   37.80   37.85   37.86
37.92   38.45
```

quantile-corrected (qm.a)

```
Min. 1st Qu.  Median    Mean 3rd Qu.
Max.

37.30   37.80   37.85   37.87   37.92
38.40
```

RCP8.5 – CHL

same observations than for RCP4.5.

Average summer CHL predicted by P.E. model (uncorrected):

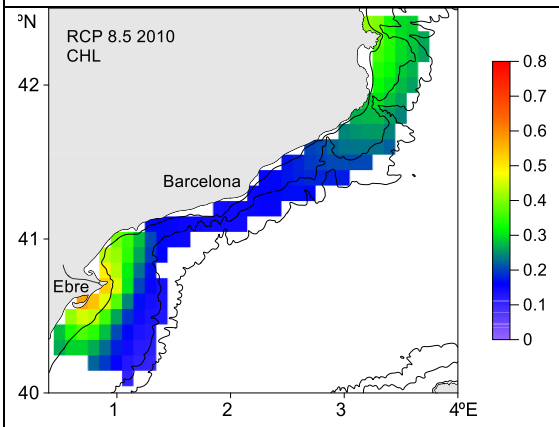

Average summer CHL predicted by P.E. model (corrected or “de-biased”):

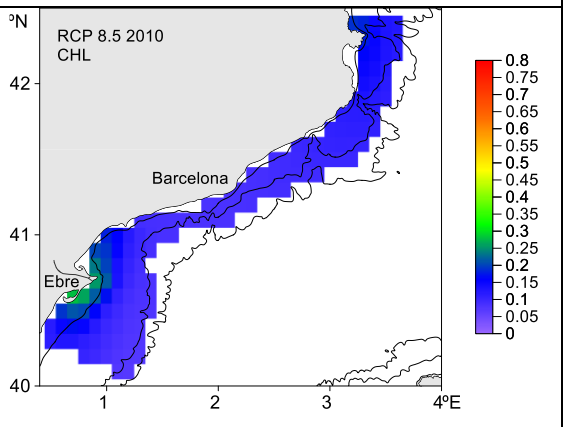

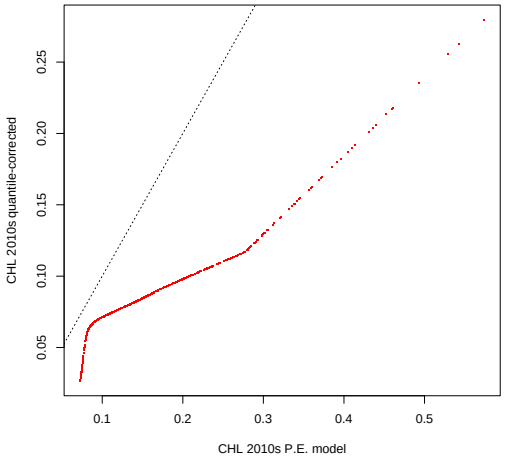

Quantiles of the 3 data sets:

```
P.E. model

Min. 1st Qu.  Median    Mean 3rd Qu.
Max.

0.0727 0.0857 0.1161 0.1514 0.1939
0.5739

Observed CHL

Min. 1st Qu.  Median    Mean 3rd Qu.
Max.

0.0294 0.0655 0.0753 0.0828 0.0979
0.2900

quantile-corrected (qm.a)

Min. 1st Qu.  Median    Mean 3rd Qu.
Max.

0.0263 0.0650 0.0755 0.0835 0.0964
0.2798
```

Annex 2 – Observed spatial distribution during “Fishjelly” summer ichthyoplankton cruises.

Two plankton cruises were carried out in the framework of the research project “Fishjelly” in June 2011 and July 2012 over a regular grid of stations (Fig. 1 of the main text and figures below). A total of 64 and 58 sampling stations, respectively, were set in each cruise over the approximately 500 km-long coast, from near the coast to the shelf break. This sampling grid has been replicated from previous research projects, and the same stations were visited in 1983-1984 and 2003-2004, with the same research vessel and sampling gear (Sabatés et al. 2018; Maynou et al. 2020). A vertical CTD profile of hydrographic variables (temperature, salinity and fluorescence) was obtained at each station. Plankton was sampled with a bongo net of 60 cm diameter and mesh size of 0.3 mm. The bongo net was hauled obliquely from a maximum depth of 200 m (or less in shallower bottoms) with a vessel speed of 2 knots. Fish eggs and larvae were stored and identified to species level and counted in the laboratory under a binocular microscope. The abundance of eggs and larvae was standardized to number / 10 m^2 for descriptive and statistical analyses.

Engraulis encrasicolus

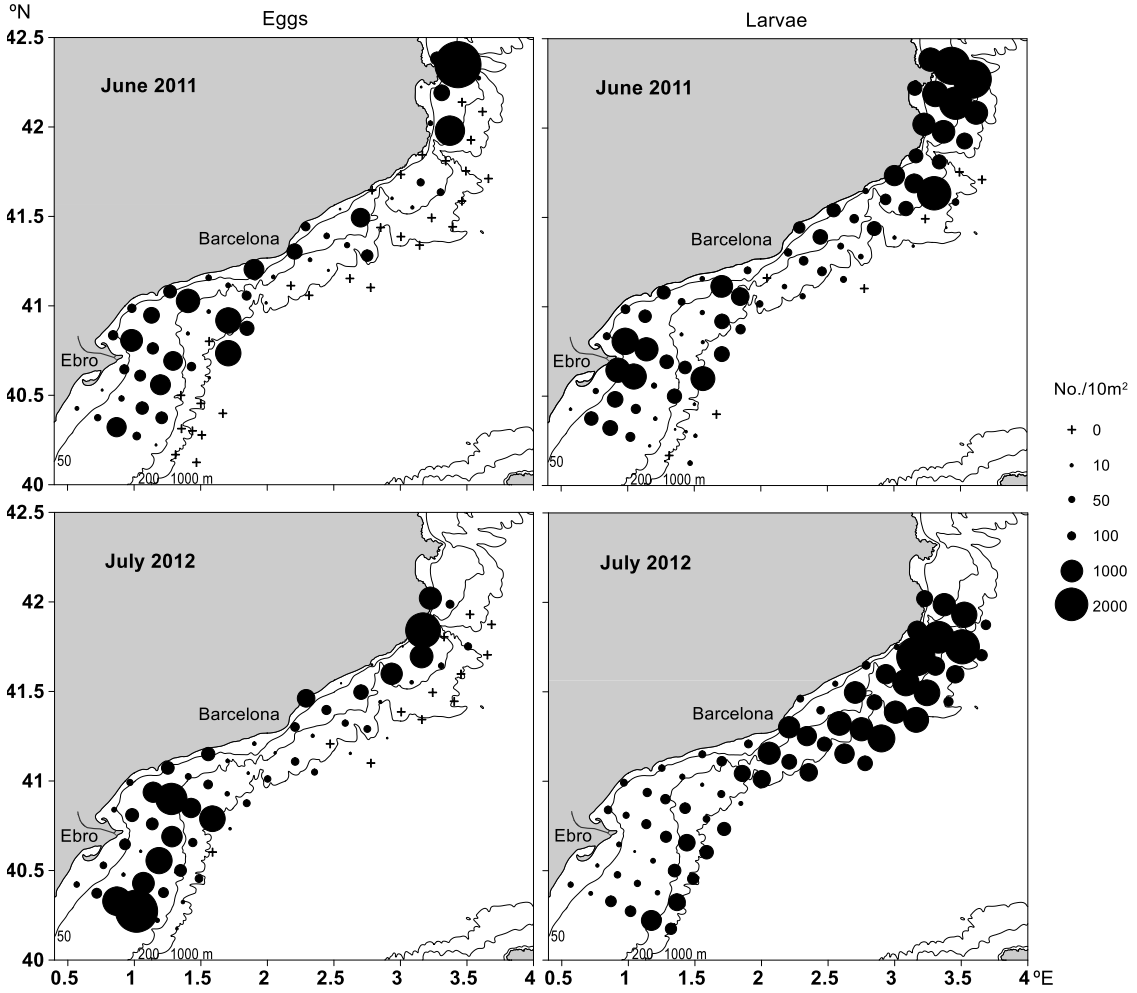

Sardinella aurita

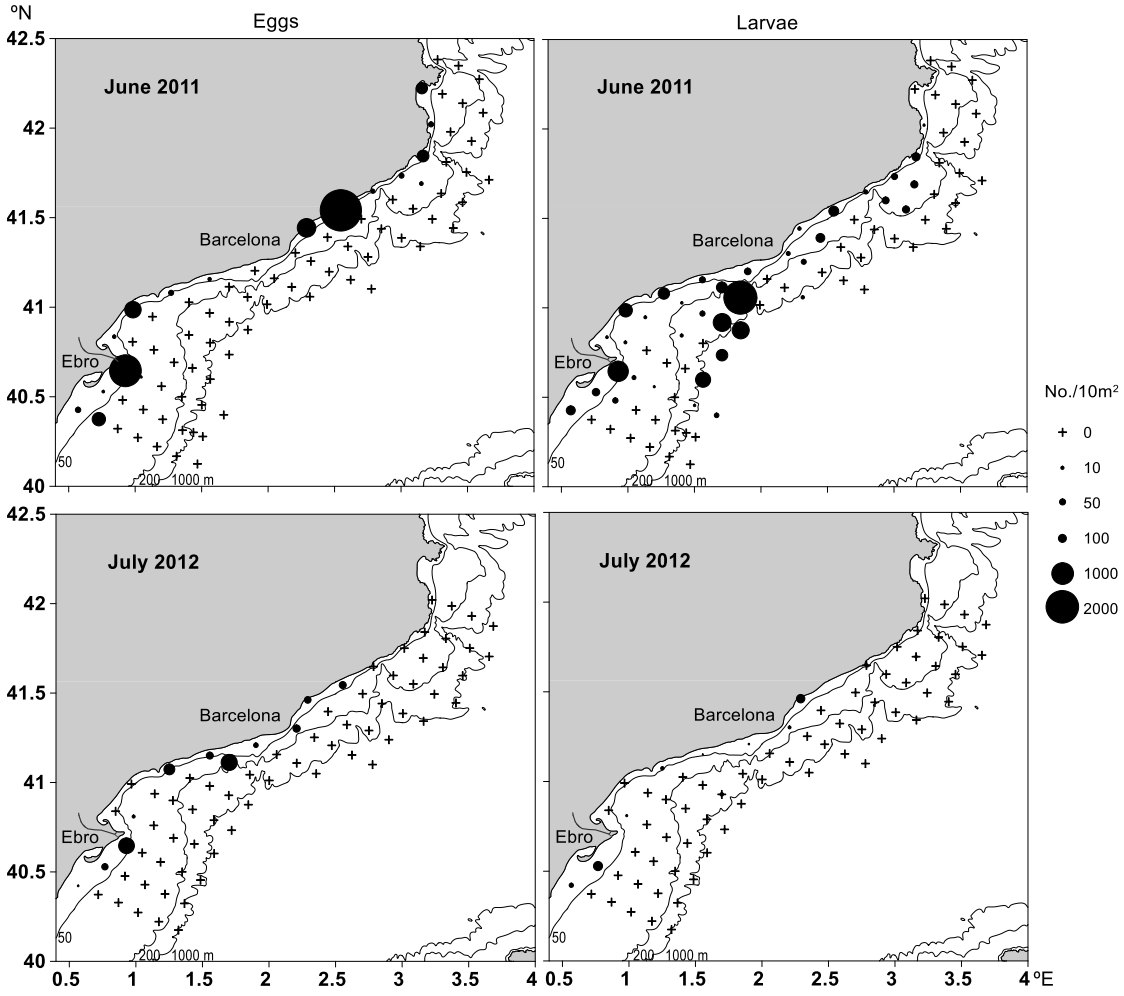

Annex 3 – Prediction of early life stages spatial distribution (2050s, 2090s)

Suitability maps for anchovy and round sardinella early life stages, computed by combining bias-corrected projected environmental variables (Fig. 3) with the statistical spatial distribution models based on GAMS (Table 1).

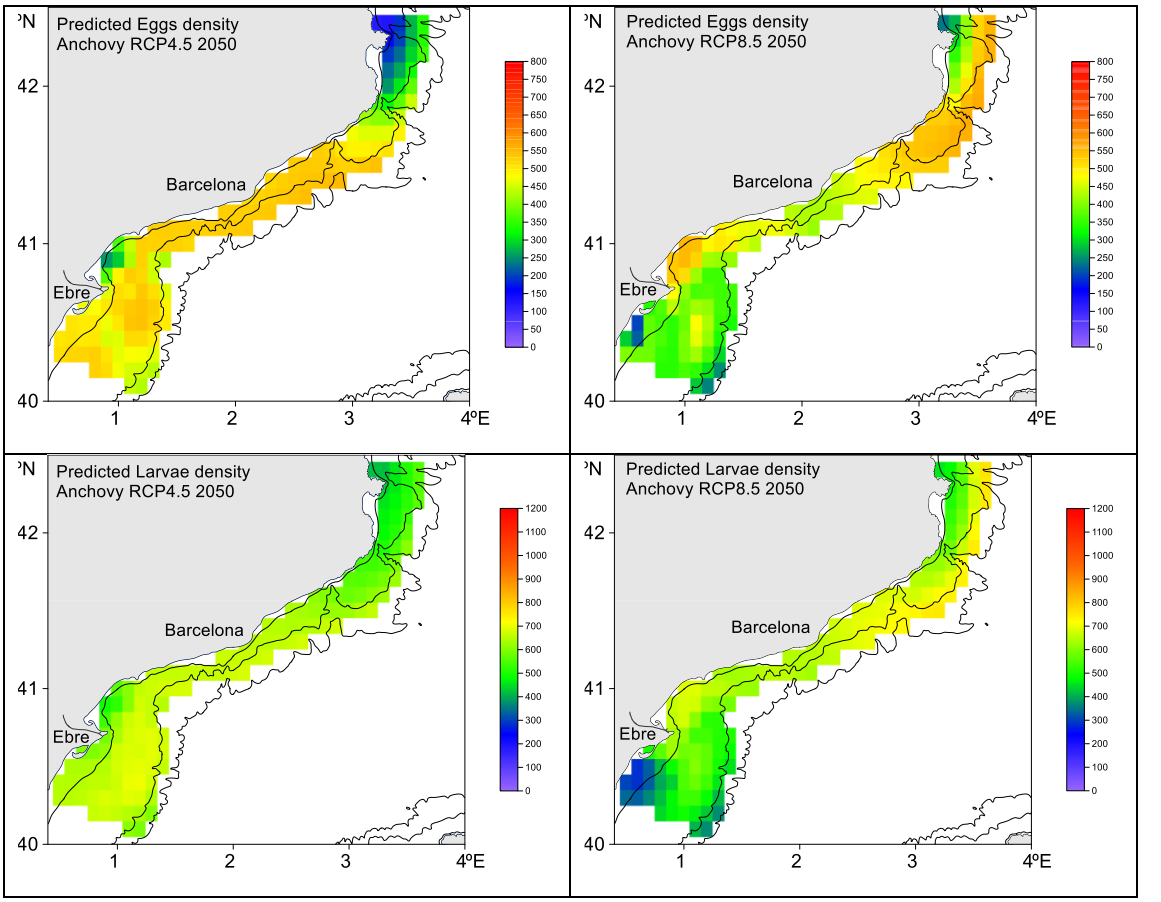

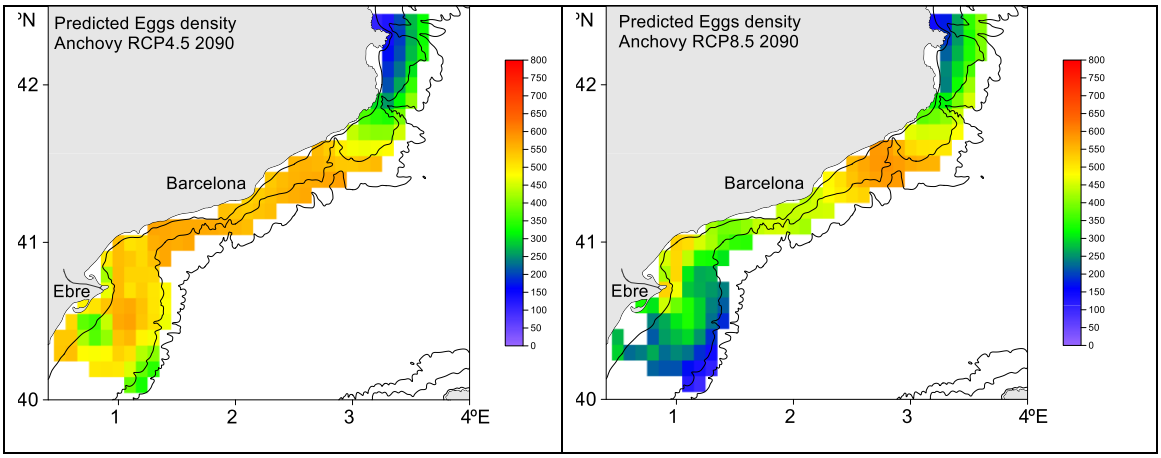

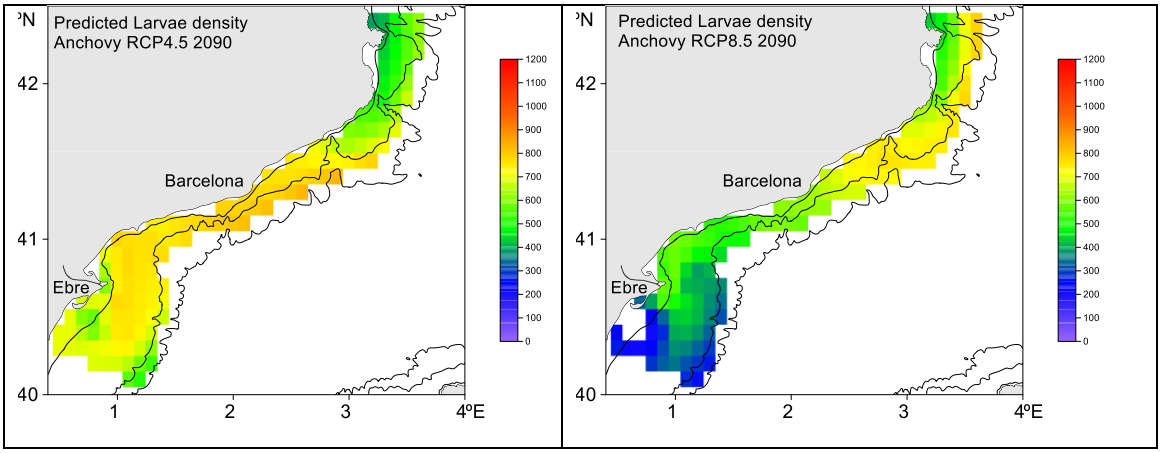
Predicted Larvae density
Anchovy RCP4.5 2090
Barcelona
Ebre
Predicted Larvae density
Anchovy RCP8.5 2090
Barcelona
Ebre

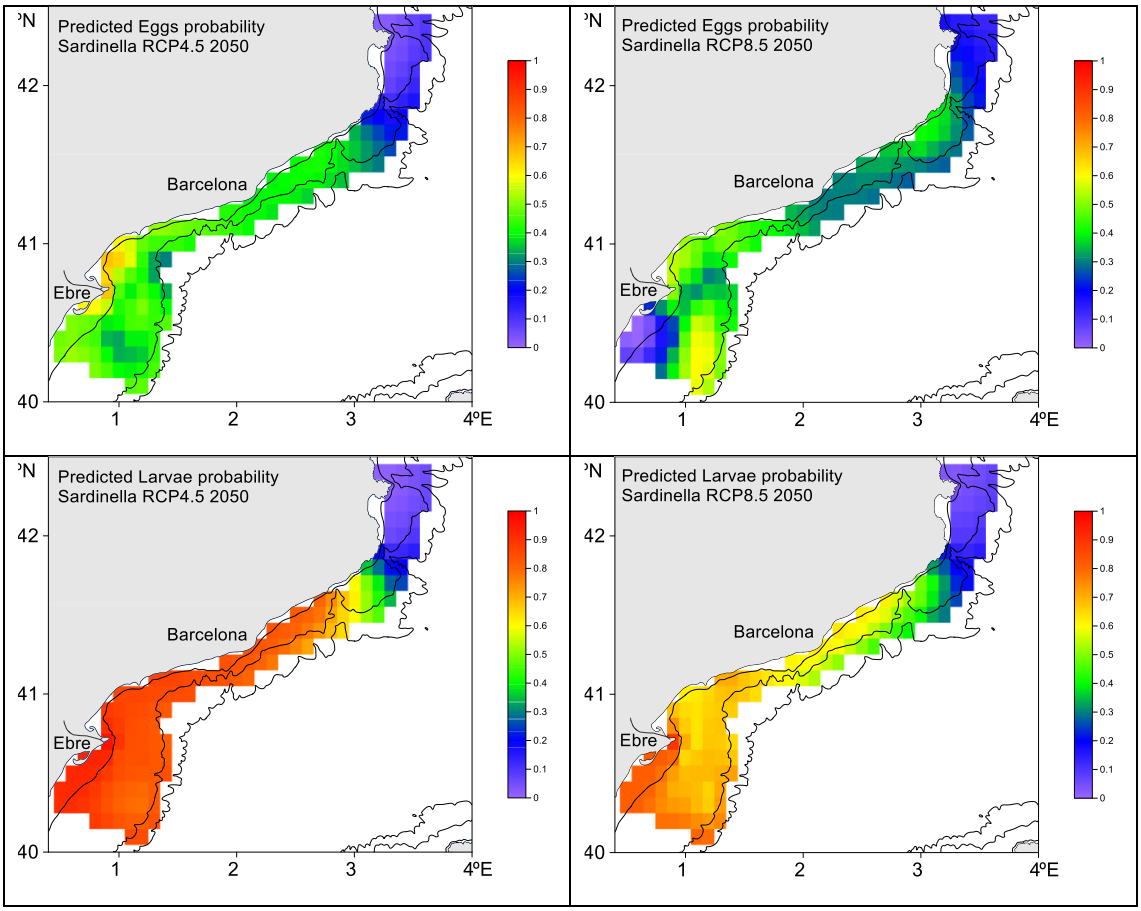
Predicted Eggs probability
Sardinella RCP4.5 2050
Barcelona
Ebre
Predicted Eggs probability
Sardinella RCP8.5 2050
Barcelona
Ebre
Predicted Larvae probability
Sardinella RCP4.5 2050
Barcelona
Ebre
Predicted Larvae probability
Sardinella RCP8.5 2050
Barcelona
Ebre

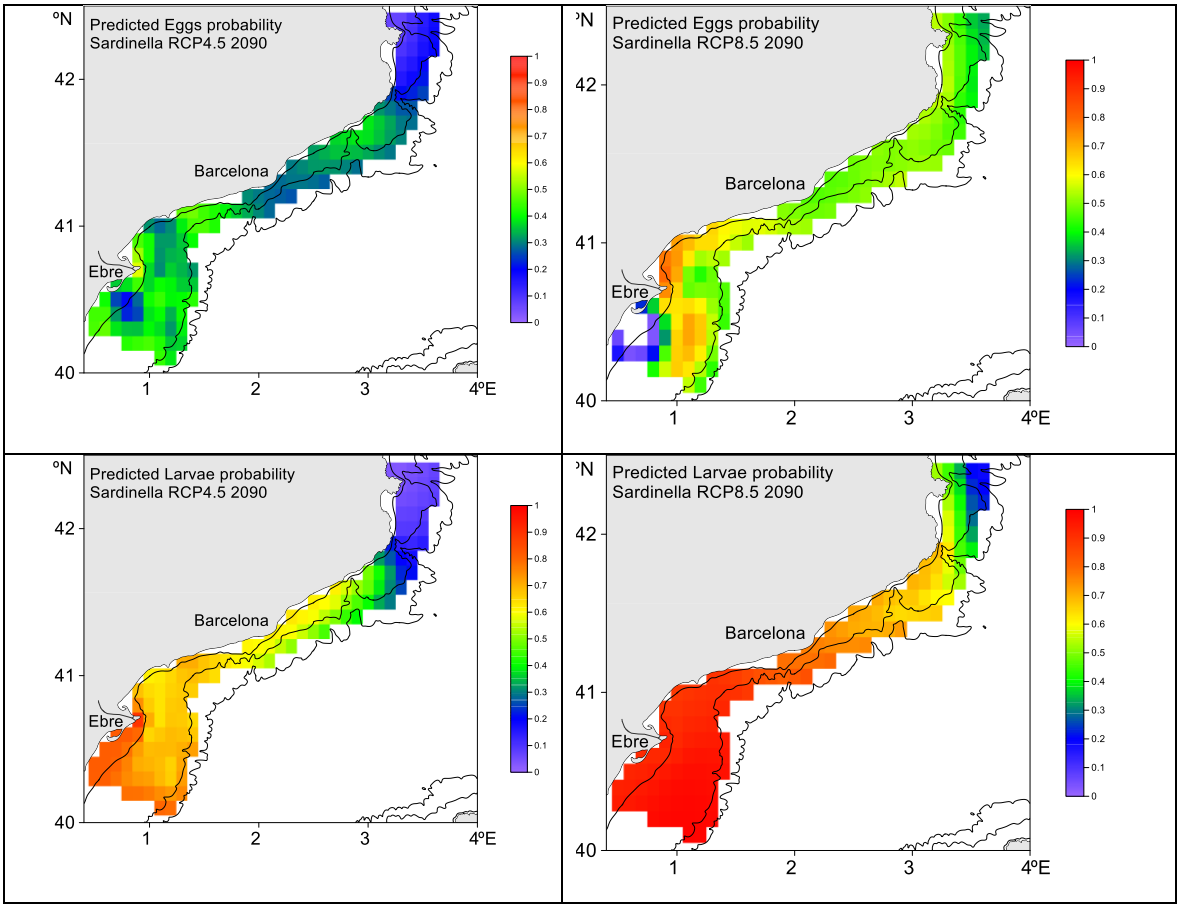
Predicted Eggs probability
Sardinella RCP4.5 2090
Barcelona
Ebre
42
41
40
1
2
3
4ºE
Predicted Eggs probability
Sardinella RCP8.5 2090
Barcelona
Ebre
Predicted Larvae probability
Sardinella RCP4.5 2090
Barcelona
Ebre
Predicted Larvae probability
Sardinella RCP8.5 2090
Barcelona
Ebre

Annex 4 – Standard Error of the Mean predictions

standard error of the mean prediction of maps in Annex 3, in the same order

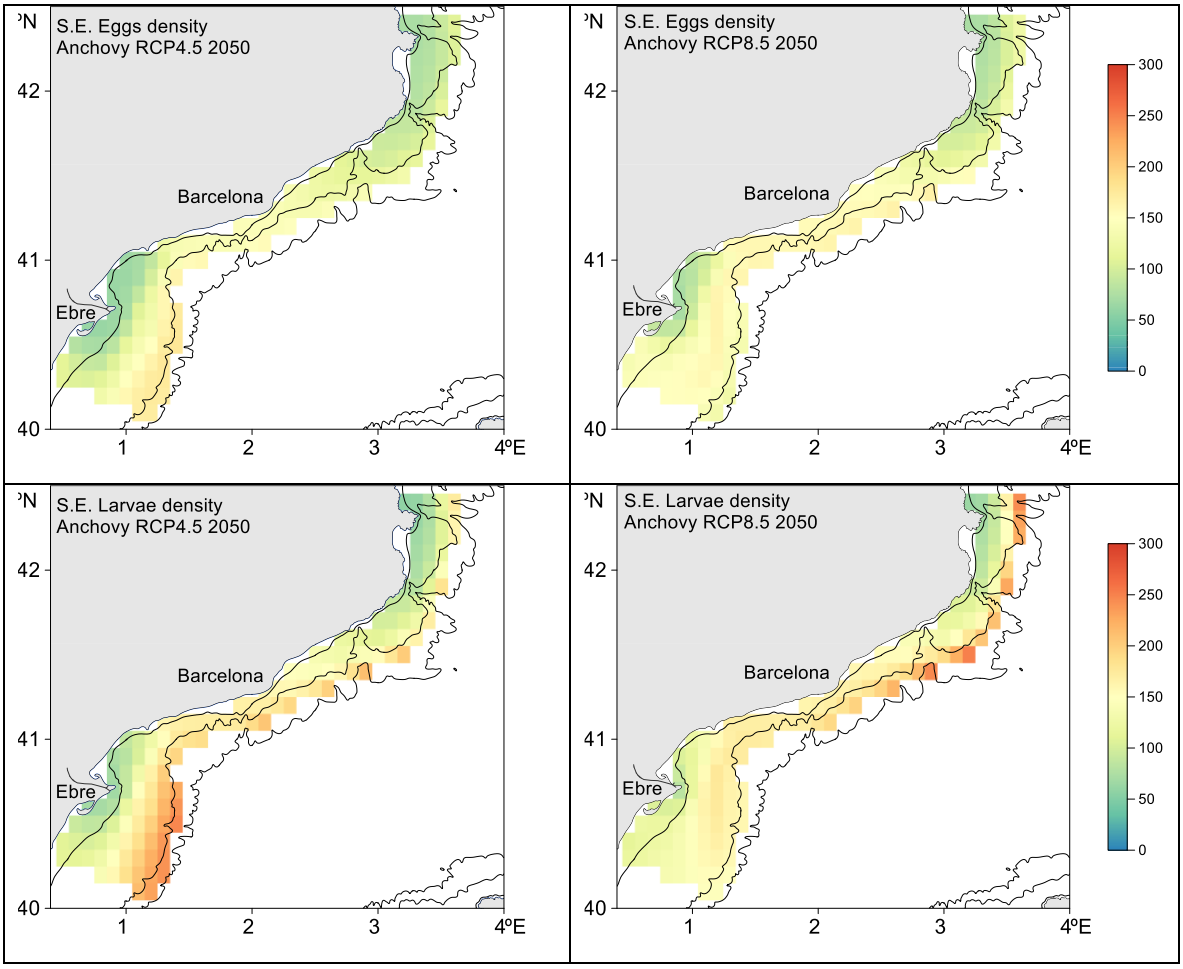

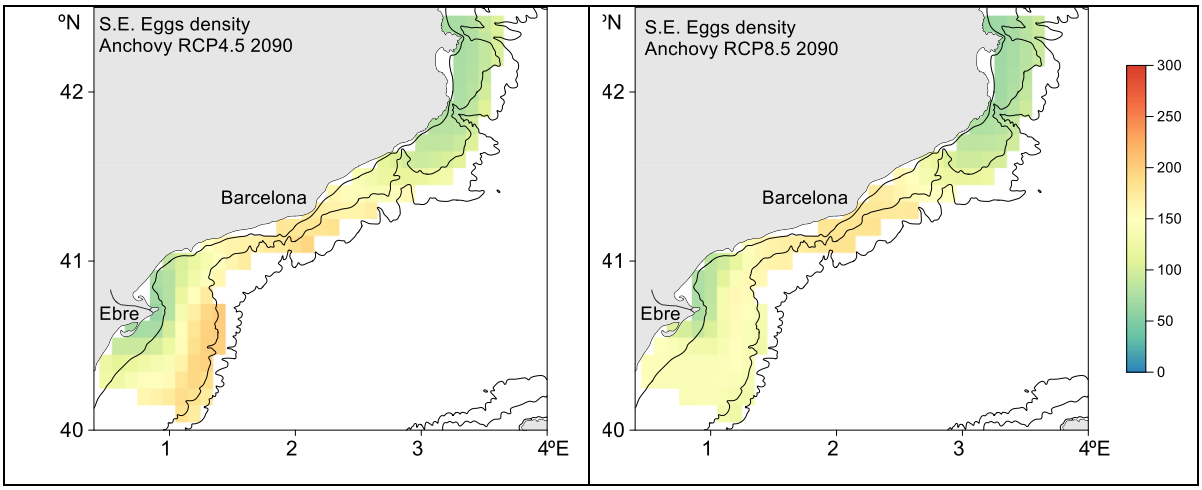

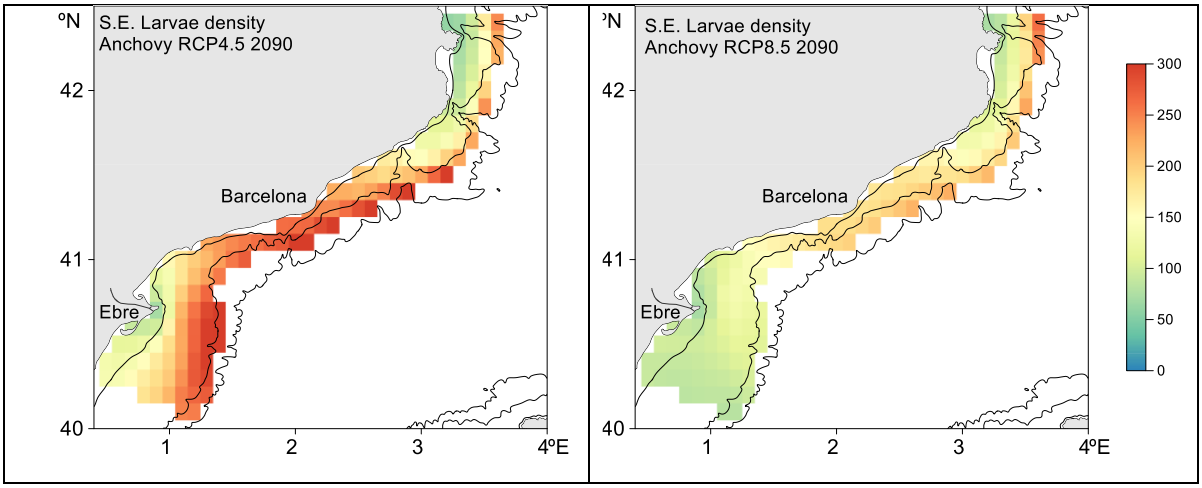
S.E. Larvae density
Anchovy RCP4.5 2090
S.E. Larvae density
Anchovy RCP8.5 2090
Barcelona
Ebre
42
41
40
1
2
3
4ºE
300
250
200
150
100
50
0

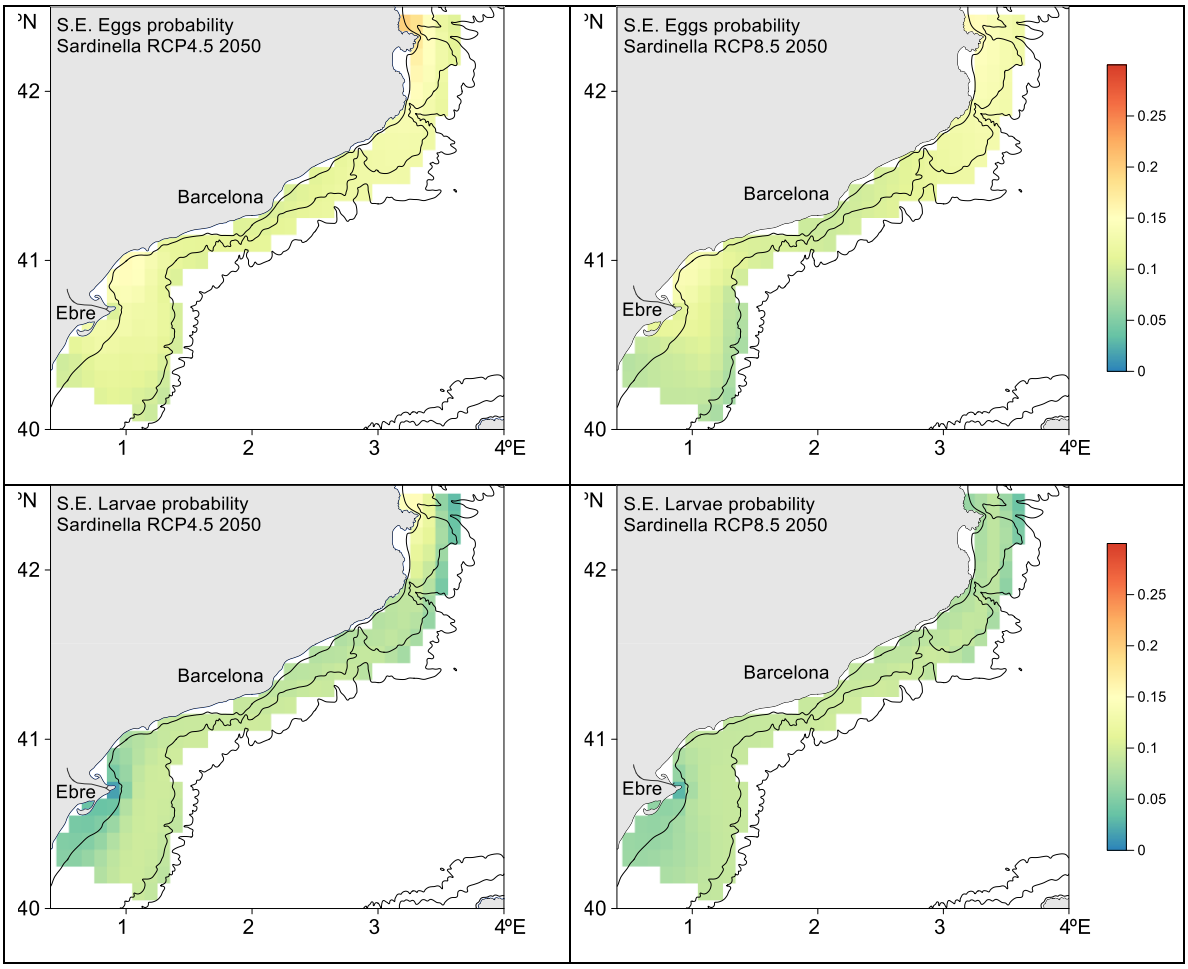
S.E. Eggs probability
Sardinella RCP4.5 2050
S.E. Eggs probability
Sardinella RCP8.5 2050
S.E. Larvae probability
Sardinella RCP4.5 2050
S.E. Larvae probability
Sardinella RCP8.5 2050
Barcelona
Ebre
42
41
40
1
2
3
4ºE
0.25
0.2
0.15
0.1
0.05
0

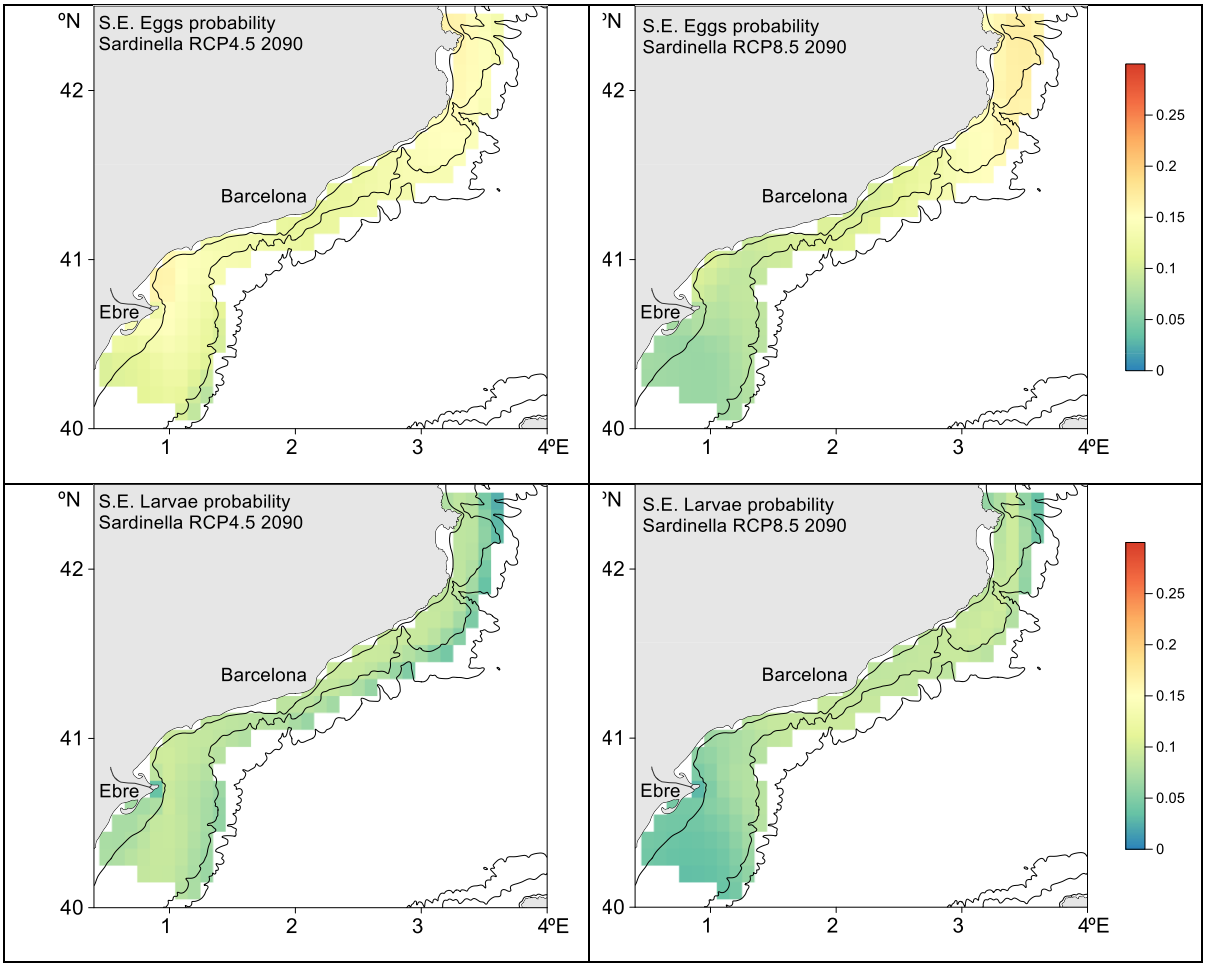
ºN
S.E. Eggs probability
Sardinella RCP4.5 2090
42
41
40
Barcelona
Ebre
1
2
3
4ºE
'N
S.E. Eggs probability
Sardinella RCP8.5 2090
0.25
0.2
0.15
0.1
0.05
0
ºN
S.E. Larvae probability
Sardinella RCP4.5 2090
'N
S.E. Larvae probability
Sardinella RCP8.5 2090